transformation produced 4.0–5.0 × 10^5 clones, we finally screened 4.30 × 10^6 colonies after 10 transformations. The cDNA-containing plasmids were recovered from the antibiotic-resistant and *lac*Z-positive clones, and the sequences of the cDNA inserts were verified, using the pTRG forward primer (5′-CAGCCTGAAGTGAAAGAA-3′) and the pTRG reverse primer (5′-ATTCGTCGCCCGCCATAA-3′), by a PRISM 310 or 3100 autosequencer. For the construction of the N-terminal Myc-tag fusion protein expression vector, a synthetic oligonucleotide containing the Myc-tag sequence, followed by HindIII, NcoI, BamHI, NotI, and EcoRI sites as multicloning sites, was ligated into pcDNA3 digested with HindIII and EcoRI to yield the plasmid pcDNA/Myc. The cDNAs of the candidate positive clones were amplified by PCR with the pTRG forward and reverse primers, digested with BamHI, NotI, or EcoRI for the 5′-junction and XhoI for the 3′-junction, and then subcloned into the corresponding sites of pcDNA3/Myc.

GST Pull-down Assay—The Myc-tagged protein encoded by the cloned cDNA was synthesized by the TnT Quick Coupled Transcription/Translation Systems (Promega) with unlabeled methionine. To construct the plasmids pGEX-hIRF-3ΔN1–3, pGEX-hIRF-3 was digested with ScaI, MscI, or BglII, blunt-ended with the Klenow enzyme, and then digested with SacII. The 938-bp ScaI-SacII fragment, the 608-bp MscI-SacII fragment, and the 350-bp BglII-SacII fragment were excised and subcloned into the blunt-ended NcoI site and the SacII site of the pGEX-hIRF-3 plasmid, respectively. To construct pGEX-hIRF-3ΔC1, the 5925-bp BglII-NotI fragment of pGEX-hIRF-3 was blunt-ended with the Klenow enzyme, and then self-ligated. To construct pGEX-hIRF-3ΔC2 and -ΔC3, the 724-bp NcoI-*Msc*I fragment and the 394-bp NcoI-ScaI fragment were excised from pGEX-hIRF-3 and then subcloned into the blunt-ended NotI site and the NcoI site of the pGEX-hIRF-3 plasmid, respectively. To create a PPIase-defective mutant of CypB, both the arginine at the 96th position and the phenylalanine at the 101st position of CypB were substituted by alanine, using the QuikChange site-directed mutagenesis kit (Stratagene). To construct the Myc-cyclophilin A (CypA) expression plasmid, the CypA cDNA was amplified by RT-PCR using PfuUltra™ DNA polymerase and the gene-specific primers (forward 5′-CGGAATTCGGCACGAGGCCATGGTCAACCCCACC-GTGTTC-3′ and reverse 5′-GCCGCTCGAGTCAAACTTATTCGAGTT-GTCCACAG-3′) with an amplification cycle of 95 °C/30 s, 62 °C/30 s and 72 °C/60 s for 25 cycles. The amplified cDNA was digested with EcoRI and XhoI, and was subcloned into the corresponding sites of pcDNA3-Myc-CypB. *E. coli* strain TG1 was transformed with each plasmid construct, and was grown in LB medium to an $A_{600} > 0.4$. After 3 h of culture in the presence of 2 mM IPTG, for the induction of fusion protein synthesis, the cells were harvested by centrifugation, resuspended in one-twelfth volume of PBS(-) containing 0.5 mM phenylmethylsulfonyl fluoride, and sonicated. The amount of protein used was adjusted on the basis of an SDS-PAGE analysis. The cleared lysates were mixed with 20 μl of glutathione-Sepharose beads for 1 h at 4 °C and subsequently were washed 3 times with DBT-0.1 (dilution buffer with Triton X) (20 mM Hepes-KOH (pH 7.9), 0.5 mM EDTA, 1 mM dithiothreitol, 20% glycerol, 0.2% Triton X-100, 100 mM KCl). The affinity beads were incubated with 150 μl of precleared *in vitro* translated protein for 2 h at 4 °C. After washing the beads 3 times with DBT-0.4 (20 mM Hepes-KOH (pH 7.9), 0.5 mM EDTA, 1 mM dithiothreitol, 20% glycerol, 0.2% Triton X-100, 400 mM KCl), the proteins retained on the beads were extracted in 20 μl of SDS-PAGE sample buffer and were separated on 4–20% SDS gradient gels (Daiichi Chemicals, Tokyo, Japan). Proteins were detected by Western blotting with a rabbit polyclonal anti-Myc antibody (Cell Signaling Technology).

Immunoprecipitation—To detect the association of endogenous IRF-3 and CypB, we performed the immunoprecipitation experiment using the human fibrosarcoma cell line, HT1080. The aliquot of cells was pelleted by centrifugation and infected with NDV for 10 min at 37 °C, and then a whole cell extract was prepared. An aliquot of each extract was incubated with 5 μg of goat IgG or goat polyclonal anti-IRF-3 antibody (C-20, Santa Cruz Biotechnology, Santa Cruz, CA) for 1 h at 4 °C. After this incubation, the protein G beads were added to the mixture and incubated for 4 h at 4 °C. The following procedures were the same as those used for the GST pull-down described above. Proteins were detected by Western blotting with a goat polyclonal anti-IRF-3 antibody (C-20) and a rabbit polyclonal anti-cyclophilin B antibody (Affinity BioReagents, Inc.).

RNA Interference—Human fibrosarcoma HT1080 cells were maintained in Dulbecco's modified Eagle's medium supplemented with 10% fetal bovine serum, 100 μg/ml penicillin, and 50 μg/ml streptomycin in a 37 °C incubator with 5% CO_2 and 100% humidity. The sense and antisense strands of the siRNAs for CypB (5′-GGUGGAGAGCAC-CAAGACATT-3′, 5′-UGUCUUGGUGCUCUCCACCTT-3′) and for the control (5′-ACAGAACCACGAGAGGUGGTT-3′, 5′-CCACCUCU-CGUGGUUCUGUTT-3′) were annealed according to the provider's instructions, respectively (JBioS, Tokyo, Japan). Cells were transfected with siRNAs using Lipofectamine 2000 (Invitrogen). In brief, 1.0 × 10^6 cells/well were seeded in a 6-well tissue culture plate. After 24 h of incubation, the medium was replaced by culture medium without antibiotics. To allow the siRNA-liposome complexes to form, 5 μl of siRNAs (20 μM) and 5 μl of Lipofectamine 2000 reagent were combined in 500 μl of Opti-MEM medium and incubated at room temperature for 20 min. This mixture was added to the cells and incubated for 24 h. The cells were then washed twice with dilution medium (Dulbecco's modified Eagle's medium containing 10% bovine serum albumin) and infected with NDV by the addition of 100 μl of allantoic fluid from NDV-infected chicken eggs (1000 hemagglutinin units/ml) for 1.5 h. After washing twice with complete medium (Dulbecco's modified Eagle's medium supplemented with 10% fetal bovine serum, 100 μg/ml penicillin, and 50 μg/ml streptomycin), the cells were further incubated in complete medium for 10.5 h before harvesting for extract preparation.

Preparation of Whole Cell Extracts—The cells were washed with ice-cold phosphate-buffered saline(−) and then scraped and suspended in 400 μl of cell lysis buffer (50 mM Tris-HCl (pH 8.0), 120 mM NaCl, 0.5% Nonidet P-40, 10% glycerol, 2 mM Na_3VO_4, 10 mM NaF, 0.2 mM phenylmethylsulfonyl fluoride). The cells were lysed by vortexing briefly, and the lysates were incubated on ice for 10 min. The whole cell extracts were recovered after centrifugation at 15,000 rpm for 10 min at 4 °C.

Western Blotting—The procedures were the same as those used in the GST pull-down experiment described above. The antibodies used were the goat polyclonal anti-IRF-3 antibody (C-20), the mouse monoclonal anti-IRF-3 Ser(P)-396 antibody (HIS5133, a gift provided by Drs. J. Hiscott and M. Servant, McGill University), the rabbit polyclonal anti-cyclophilin B antibody, and the mouse monoclonal anti-actin antibody (Chemicon).

Native PAGE Assay—The native PAGE assay was performed by using 7.5% polyacrylamide gels (Daiichi Chemicals). The gel was prerun in a running buffer containing 25 mM Tris and 192 mM glycine, with and without 1% deoxycholate in the cathode and anode chambers, respectively, for 30 min at 40 mA. Aliquots of whole cell extracts were diluted in native sample buffer (62.5 mM Tris-HCl (pH 6.8), 15% glycerol, and 1% deoxycholate), applied to the gel, and electrophoresed for 60 min at 25 mA. Immunoblotting was performed as described above. Proteins were detected by Western blotting with a goat polyclonal anti-IRF-3 antibody (C-20) or a rabbit polyclonal anti-IRF-3 Ser(P)386 antibody (IBL).

Electrophoretic Mobility Shift Assay—To examine the binding of IRF-3 to the IFN-β promotor, an electrophoretic mobility shift assay was performed using whole cell extracts from siRNA-transfected and NDV-infected or -uninfected HT1080 cells. The extracts were incubated in a reaction buffer (25 mM Tris-HCl (pH 8.0), 60 mM NaCl, 0.25% Nonidet P-40, 5% glycerol, 1 mM Na_3VO_4, 5 mM NaF, 1 mM dithiothreitol, 100 mg/ml poly(dI-dC)). After a 30-min incubation on ice, ~10,000 cpm of a ^{32}P-labeled double-stranded oligonucleotide containing the ISRE sequence of the ISG15 gene (5′-GGGAAAGGGAAACCGAAACT-GAA-3′) were added to the reactions, which were then incubated for an additional 30 min at 25 °C. The reactions were further incubated with an anti-IRF-3 antibody (C-20) or an anti-CBP antibody (A-22X) (Santa Cruz Biotechnology) for 30 min at 25 °C. The binding reactions were mixed with 1 μl of loading buffer (0.1% bromphenol blue in the same buffer used for the binding reactions) and then were electrophoresed on a nondenaturing 4% polyacrylamide gel with 0.5 × TBE (Tris borate-EDTA) at 200 V for 2 h. The gel was dried and analyzed by an image analyzer, BAS5000 (Fuji, Tokyo).

Chromatin Immunoprecipitation Assay—HT1080 cells were mock- or NDV-infected for 12 h and then treated with formaldehyde to cross-link the proteins bound to DNA. The cross-linked proteins were purified and immunoprecipitated with the anti-IRF-3 antibody (C-20). After reversal of the cross-linking, the DNA was amplified using primers for the ISG15 promoter (5′-TTTTCCCTGTCTTTCGGTCATTCG-3′, 5′-TAT-TATAAGCCTGAGGCACACACG-3′) with an amplification cycle of 94 °C/1 min, 55 °C/1 min, and 72 °C/2 min for 30 cycles.

Enzyme-linked Immunosorbent Assay for IFN-β—The amounts of human IFN-β in the culture medium supernatants before and after NDV infection were quantified with a human interferon-β enzyme-linked immunosorbent assay kit (R&D Systems). Data are expressed as the mean ± S.D. Differences among groups were examined for statistical significance using one-factor analysis of variance (Bonferroni/Dunn). A p value < 0.05 denoted the presence of a statistically significant difference.

RESULTS

Isolation of Putative IRF-3-binding Proteins by the Bacterial Two-hybrid Screening—To isolate the protein(s) that associate with IRF-3, we performed a screening by a bacterial two-hybrid system (16, 17). The bait was fused to the full-length bacteriophage λ repressor protein (λ*cI*), whereas the corresponding target protein was fused to the N-terminal domain of the α-subunit of RNA polymerase. When the bait and target interact, they recruit and stabilize the binding of RNA polymerase at the promoter and activate the transcription of reporter genes, the carbenicillin-resistance and the β-galactosidase genes. In addition, this system offers the ability to detect an interaction between a pair of protein domains with an equilibrium dissociation constant in the high nanomolar range. In the present study, we used IRF-3 as the bait and a human HeLa cell cDNA library as the target. We obtained 272 antibiotic-resistant and *lac*Z-positive clones from 4.30×10^6 screened clones. To identify the protein encoded by the candidate positive clones, the nucleotide sequence of each clone was determined. Among the clones obtained, only 25 clones encoded in-frame fusion proteins to the λ*cI* repressor. These clones were used in a search for homology in the NCBI data base. The cDNA fragments of the positive clones were subcloned into an expression vector to produce N-terminally Myc-tagged fusion proteins. However, we obtained *in vitro* coupled transcription/translation products from only 13 of 25 clones. For these 13 clones, we performed a GST pull-down assay to confirm their binding activities to IRF-3. Only clone A25 (cyclophilin B) showed specific binding to IRF-3 (data not shown). Therefore, we concentrated our efforts on the interaction between IRF-3 and CypB.

Mapping the IRF-3 and Cyclophilin B Interaction Domains—To confirm the specificity of the interaction between IRF-3 and CypB, we examined which region of IRF-3 is important for binding to CypB. A GST pull-down assay was performed with a series of IRF-3 deletion mutants fused to GST and *in vitro* translated full-length CypB (Fig. 1*A*). As mentioned above, CypB bound to GST-IRF-3 but not to GST alone (Fig. 1*B*, *lanes 3* and *2*). The deletion of the N-terminal DNA-binding domain somehow enhanced the binding of CypB (Fig. 1*B*, *lane 4*), whereas further removal of the nuclear export signal and the proline-rich region reduced the affinity to CypB (*lane 5*). Unexpectedly, the deletion of the IAD restored the interaction potential of IRF-3 to CypB (Fig. 1*B*, *lane 6*). When we removed the C-terminal 296 residues from IRF-3, the interaction with CypB was not detected (Fig. 1*B*, *lane 9*). It is noteworthy that the mutants ΔN3 and ΔC1 do not share any regions of IRF-3 but still exhibited the CypB binding, suggesting that IRF-3 has multiple sites for CypB binding. Furthermore, the IAD seems to have an inhibitory effect on the binding, as the binding of ΔN2 is weaker than that of ΔN3, the construct lacking two thirds of the IAD from ΔN2. We did not perform a GST pull-down analysis with GST-CypB to detect the binding with IRF-3, because the GST-CypB expression plasmid failed to produce a detection level of the protein in *E. coli*.

Next, we examined the regions of CypB required for the interaction with IRF-3. Because CypB is a rather small protein (208 amino acids), even a small deletion drastically destabilized the mutant forms of the protein (data not shown). Thus, we tested whether the PPIase activity of CypB, a well known biological activity of the protein, was required for the binding to IRF-3. For this purpose, arginine 96 and phenylalanine 101 in the PPIase domain of CypB were substituted with alanines by site-directed mutagenesis (Fig. 1*C*). As shown in Fig. 1*D*, the PPIase mutant did not bind to IRF-3 (*lane 9*). In addition, we found that cyclophilin A (CypA), the most abundant cyclophilin *in vivo*, could not bind to IRF-3 (*lane 3*).

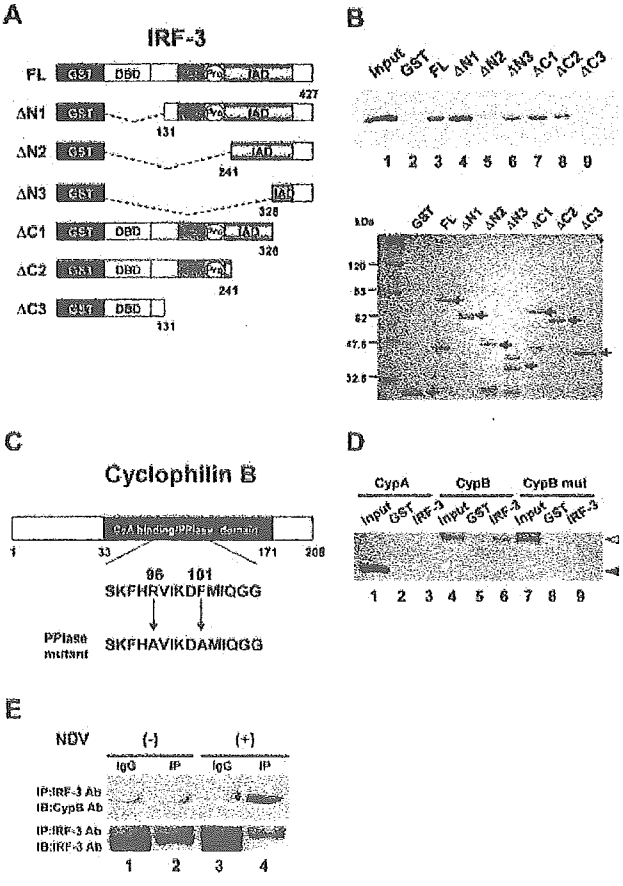

FIG. 1. **Mapping the interaction domains of IRF-3 and CypB.** *A*, schematic representation of IRF-3 deletion mutants. Structures of wild type (*top*) and deletion mutants (ΔN1–3 and ΔC1–3) of IRF-3 are shown. Locations of functional domains are indicated. *DBD*, DNA-binding domain; *NES*, nuclear export signal; *Pro*, proline-rich region; *IAD*, interferon-associated domain. *B*, GST pull-down assay between IRF-3 mutants and CypB. *Input*, 5% of *in vitro* translated Myc-tagged CypB was included in the binding reactions. *GST*, GST protein only (not fused with IRF-3); *FL*, GST fusion of wild type IRF-3 protein; *ΔN1*, GST fusion of IRF-3 truncated 131 residues from the N terminus; *ΔN2*, GST fusion of IRF-3 truncated 241 residues from the N terminus; *ΔN3*, GST fusion of IRF-3 truncated 328 residues from the N terminus; *ΔC1*, GST fusion of IRF-3 truncated 99 residues from the C terminus; *ΔC2*, GST fusion of IRF-3 truncated 186 residues from the C terminus; *ΔC3*, GST fusion of IRF-3 truncated 296 residues from the C terminus. *C*, schematic representation of cyclophilin B PPIase mutants. The wild type CypB structure (*top*) is shown. The amino acid sequence of the wild type CypB and the mutated residues are shown. *CsA*, Cyclosporin A. *D*, GST pull-down assay between CypB, CypB PPIase mutant, or CypA and wild type IRF-3. *Input*, 5% of *in vitro* translated Myc-tagged CypB, Myc-tagged CypB PPIase mutant, or Myc-tagged CypA was included in the binding reactions, respectively. *GST*, GST protein only (not fused with IRF-3); *IRF-3*, GST-fusion of wild type IRF-3 protein. The *solid* and *empty arrowheads* indicate CypB and CypA, respectively. *E*, co-immunoprecipitation assay to detect an endogenous association between IRF-3 and CypB *in vivo*. Whole cell lysates prepared from cells, either mock-infected or NDV-infected for 10 min, were used as the input. *IgG*, lysates incubated with goat IgG (*lanes 1* and *3*) *IP*, lysates incubated with goat polyclonal anti-IRF-3 antibody (C-20) (*lanes 2* and *4*). *IB*, immunoblot. The data are representative of three independent experiments.

Then, we examined the interaction between IRF-3 and CypB *in vivo*. The association of endogenous IRF-3 and CypB was detected when an anti-IRF-3 antibody was used for the precipitation of an extract prepared 10 min after NDV infection (Fig. 1*E*, *lane 4*) but not 30 min after the infection (data not shown). On the other hand, the available anti-CypB antibodies could

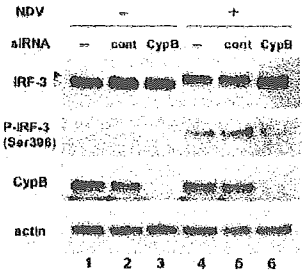

FIG. 2. **Cyclophilin B knockdown inhibits virus-induced IRF-3 phosphorylation.** HT1080 cells were mock-transfected (*lanes 1* and *4*) or transfected with control siRNA (*lanes 2* and *5*) or CypB siRNA (*lanes 3* and *6*), respectively, followed by mock infection (*lanes 1–3*) or infection with NDV for 12 h (*lanes 4–6*). Whole cell extracts were prepared and subjected to immunoblotting using the anti-IRF-3 (C-20) antibody (*first panel*), the anti-IRF-3 Ser(P)-396 antibody (*second panel*), the anti-CypB antibody (*third panel*), or the anti-actin antibody (*fourth panel*). The *solid* and *empty arrowheads* indicate the phosphorylated IRF-3 and the unphosphorylated IRF-3, respectively. The data are representative of three independent experiments.

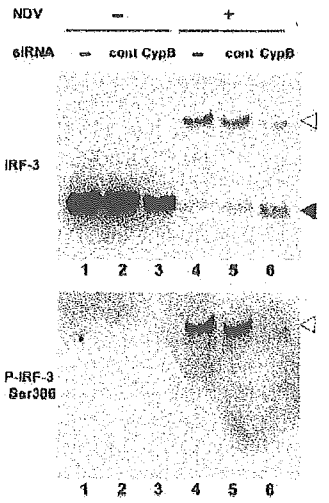

FIG. 3. **Cyclophilin B knockdown inhibits virus-induced IRF-3 dimerization.** Whole cell extracts were prepared as described in Fig. 2 and were analyzed by native PAGE followed by immunoblotting with the anti-IRF-3 (C-20) antibody (*upper panel*) and the anti-IRF-3 Ser(P)-386 antibody (*lower panel*). The *solid* and *empty arrowheads* indicate the monomer and the dimer of IRF-3, respectively. The data are representative of three independent experiments.

not precipitate the endogenous IRF-3 with CypB, even 10 min after the infection. We also tried to characterize the binding domains of IRF-3 with CypB by using mutant IRF-3 expression plasmids. Unfortunately, the IRF-3 expression was inhibited when the CypB plasmid was introduced simultaneously. This is consistent with previous reports that CypB may participate in inducing the degradation of exogenously introduced DNA (18, 19).

Cyclophilin B Is Required for Virus-induced Phosphorylation of IRF-3—To examine the physiological roles of CypB in the IRF-3 function, we performed RNA interference experiments to knock down CypB *in vivo* and then examined the biochemical activities of IRF-3 after NDV infection. As shown in Fig. 2, the expression of CypB was almost completely suppressed by the specific siRNA interference (*lanes 3* and *6*, *third panel*). NDV infection in the mock- or control siRNA-transfected cells resulted in a mobility shift of IRF-3, which reflected the C-terminal phosphorylation of IRF-3 (Fig. 2, *lanes 4* and *5*, *first panel*) (9, 20). However, IRF-3 showed an intermediate mobility in CypB siRNA-transfected/NDV-infected cells (Fig. 2, *lane 6*, *first panel*). When the same blot was reprobed with an antibody that specifically recognized a phosphorylated form of IRF-3 (21), we found that the amounts of phosphorylated IRF-3 (phosphorylated Ser-396) were reduced in the CypB siRNA-transfected cells, as compared with the mock- or control siRNA-transfected cells (Fig. 2, compare *lanes 6* with *lanes 4* and *5*, *second panel*). These results strongly suggest that the knockdown of CypB resulted in the defect in IRF-3 phosphorylation by virus infection.

The Cyclophilin B Knockdown Inhibited Virus-induced IRF-3 Dimerization—It is known that the phosphorylation of IRF-3 is prerequisite for the dimerization of IRF-3 (7, 20). We thus examined the virus-induced dimerization of IRF-3 in siRNA-transfected cells. To do this, we used the native PAGE assay that sensitively detects the difference between the monomer and dimer forms of IRF-3 (22). IRF-3 existed as a monomer in the mock-, control siRNA-, and CypB siRNA-transfected cells in the absence of NDV infection (Fig. 3, *lanes 1–3*). Upon viral infection, the monomer signals were reduced, but newly formed dimer signals were detected in the mock- and control siRNA-transfected cells (Fig. 3, *lanes 4* and *5*). However, significant amounts of the IRF-3 monomer still remained in the CypB siRNA-transfected/NDV-infected cells (Fig. 3, *lane 6*). These results clearly indicated that the specific knockdown of CypB by RNA interference inhibited the IRF-3 dimer formation induced by viral infection. The importance of CypB was again demonstrated in the phosphorylation of Ser-386, which is the critical residue in IRF-3 activation (23). CypB siRNA-transfected/NDV-infected cells failed to phosphorylate Ser-386 (Fig. 3, *panel 2*, *lane 6*).

The Cyclophilin B Knockdown Inhibited IRF-3 Binding to the ISRE and Association with CBP—Phosphorylated IRF-3 undergoes homodimerization (6, 7) and associates with the coactivators CBP/p300 (6, 9). The holocomplex has the ability to specifically recognize the target DNA sequence, called the ISRE (5, 8, 9). We examined the effects of CypB on IRF-3 in terms of the DNA binding to the ISRE and the association with the CBP/p300 coactivator, using electromobility shift assay. In the absence of NDV infection, no DNA-protein complex was observed in the mock-, control siRNA-, and CypB siRNA-transfected cells (Fig. 4, *lanes 1*, *6*, and *11*). NDV infection induced the formation of a DNA-protein complex bound to the ISRE of the ISG15 gene in the mock- and control siRNA-transfected cell extracts (Fig. 4, *lanes 2* and *7*). The addition of specific antibodies against IRF-3 to the binding reactions reduced the amount of the complex band and the induction of supershifted bands, indicating that the complex contained IRF-3 (Fig. 4, *lanes 3* and *8*). The addition of specific antibodies against CBP to the binding reactions reduced the amount of the complex but did not induce the formation of supershifted bands, indicating that complex formation was partly blocked by the antibody (Fig. 4, *lanes 4* and *9*). This is consistent with the previous result that CBP/p300 is involved in the holocomplex of IRF-3 (6–9). However, the knockdown of CypB severely impaired the DNA binding activity of IRF-3 (Fig. 4, *lane 12*). Thus, the inhibition of CypB also resulted in reduced holocomplex formation, which is required for the target gene activation by IRF-3. A chromatin immunoprecipitation analysis showed the *in vivo* binding of IRF-3 to the ISG15 promoter in NDV-infected cells (Fig. 4*B*, *lane 8*) but not in uninfected cells (Fig. 4*B*, *lane 2*). When NDV-infected cells were pretreated with CypB siRNA, the binding was significantly reduced, and no band was detected after 30 PCR cycles (Fig. 4*B*, *lane 12*), although a band was visible after 40 cycles (data not shown). The control siRNA could not reduce the binding (Fig. 4*B*, *lane 10*).

The Cyclophilin B Knockdown Reduced IFN-β Production by Newcastle Disease Virus Infection—Finally, we examined the

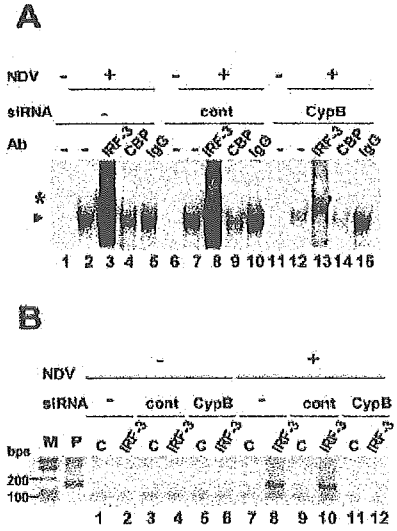

FIG. 4. **Cyclophilin B knockdown inhibits IRF-3 binding to the ISRE and association with CBP.** *A*, whole cell extracts were prepared as described in Fig. 2, and were subjected to electromobility shift assay, using the ISRE of the ISG15 gene as a probe, in the absence (*lanes 1, 2, 6, 7, 11,* and *12*) or presence of the anti-IRF-3 (C-20) antibody (*lanes 3, 8,* and *13*), the anti-CBP antibody (*Ab*) (*lane 4, 9,* and *14*), or control (*cont*) IgG (*lanes 5, 10,* and *15*). The *arrowhead* indicates the IRF-3-containing complex. The *asterisk* indicates the bands supershifted by the anti-IRF-3 antibody. *B*, chromatin immunoprecipitation assay to assess the amounts of IRF-3 bound to ISG15 promoter. *M*, marker; *P*, positive control of genomic DNA. Whole cell extracts prepared as described in Fig. 2 were subjected to the assay, using the promoter region of the ISG15 gene as primers. Each extract was immunoprecipitated with the control IgG (*C*) (*lanes 1, 3, 5, 7, 9,* and *11*) or the anti-IRF-3 (C-20) antibody (*lanes 2, 4, 6, 8, 10,* and *12*). The data are representative of three independent experiments.

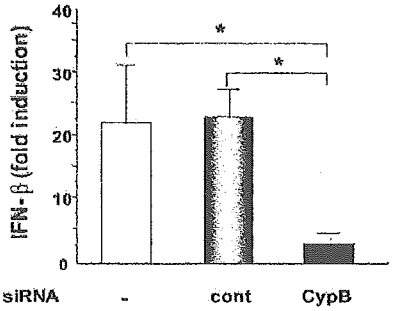

FIG. 5. **Cyclophilin B knockdown reduces IFN-β production by Newcastle Disease Virus infection.** HT1080 cells were mock-transfected, or transfected with control siRNA or CypB siRNA. After 24 h, the cells were infected with NDV for 12 h. The supernatants before and after NDV infection were analyzed by an IFN-β enzyme-linked immunosorbent assay. The results shown are the averages of three independent experiments, with S.E. *bars*. The *asterisk* indicates a p value < 0.05.

effect of CypB on the regulation of IFN-β production. The amount of IFN-β in the culture medium was assayed by enzyme-linked immunosorbent assay, before and after NDV infection. The virus infection induced a more than 25-fold activation of IFN-β in the mock- and the control siRNA-transfected cells. The CypB-siRNA treatment caused a severe defect in the viral-dependent activation of IFN-β. (Fig. 5). These results indicate that CypB is required for the efficient activation of IFN-β production upon viral infection.

DISCUSSION

We have described a novel interaction between IRF-3 and CypB. The present *in vitro* analysis suggests that autoinhibition domain of IRF-3 and the catalytic domain bearing the peptidyl-prolyl isomerase activity of CypB are required for the interaction.

CypB, a member of the cyclophilins, possesses a *cis-trans* peptidyl-prolyl isomerase activity (15). Via their PPIase activity, cyclophilins facilitate protein folding and have been shown to contribute to the maturation and trafficking of several proteins (24). Furthermore, cyclophilins regulate signal transduction cascades, as revealed by their modulation of transforming growth factor-β signaling and the transactivation of c-myb and IRF-4 (25, 26). Among the cyclophilins, CypB is distinguished from the others by the presence of an endoplasmic reticulum-directed signal sequence (15). However, CypB is found not only in the endoplasmic reticulum but also in the extracellular space and the nucleus (15). CypB has been reported to interact with prolactin. The proximal action of prolactin is mediated by its cell surface receptor. PRL activity, however, is also associated with the internalization and translocation of this hormone into the nucleus. To retrotransport it to the nucleus, and to potentiate prolactin-induced proliferation, the interaction with CypB with its PPIase activity is essential (27, 28). Similar to the interaction with prolactin, the PPIase domain of CypB is required for IRF-3 binding in a GST pull-down assay. We also found that retaining either one of the autoinhibition domains of IRF-3 is required for the binding. Previously, Mamane *et al.* (29) reported the interaction between IRF-4, a member of the IRFs, and FKBP52, another member of the immunophilins. They demonstrated that IRF-4 would not co-immunoprecipitate with FKBP52 unless the C-terminal autoinhibition domain of IRF-4 was removed. This observation raises the possibility that the interactions of immunophilins with IRF family proteins are sensitive to the conformations or the ternary structures of IRFs.

As demonstrated by our RNA interference analysis, the specific knockdown of CypB *in vivo* resulted in the inhibition of virus-induced IRF-3 activation. This was confirmed at multiple steps, including phosphorylation, dimerization, DNA binding, coactivator binding, and IFN-β-induction. If the phosphorylation of IRF-3 is a prerequisite for the following events after the virus-induced activation of IRF-3, then it is likely that CypB is involved in the phosphorylation reaction of IRF-3. The early involvement of CypB is supported by the notion that the *in vivo* association of CypB with IRF-3 was only detected 10 min after the infection but not after 30 min. At present, it has been reported that the C-terminal phosphorylation of IRF-3 is mediated by IκB kinase-ε and TANK-binding kinase 1 (10, 11). The mutagenesis of IRF-3 revealed key residues for virus-induced activation. Substitutions of the serine residues at 385 or 386 to alanine, glutamic acid, or aspartic acid made the molecule unresponsive to stimuli (7, 21). Substitutions of other serine/threonine residues, present at positions 396, 398, 402, 404, and 405, to aspartic acid made IRF-3 constitutively active (20). Recently, Servant *et al.* (21) identified Ser-396 and Ser-398 as the minimal phosphorylation sites critical for activation, based on their observation that S396D and S396D/S398D are constitutively active. More recently, Mori *et al.* (23) identified Ser-386 as the target of IRF-3, using an antibody that specifically detects the phosphorylation of Ser-386. As protein kinases are often associated with, in addition to their regulators, molecular chaperones that sometimes need to exert their specificity for the substrates, it is interesting to speculate that CypB associates with the IRF-3 kinases, IκB kinase-ε and TANK-binding kinase 1, in a similar manner. Although it will be important in the future to determine whether it is the CypB binding, catalytic activity, or both that is responsible for its effect on IRF-3, our results indicate that CypB plays a significant role in modulating IFN-β gene expression via its interaction with IRF-3.

Acknowledgments—We thank Dr. K. Yamamoto (The Chemo-Sero-Therapeutic Research Institute) for providing NDV stocks. We also thank the Division of Functional Genomics, Center for Frontier Life Sciences, Nagasaki University, for the autosequencing. We thank Dr. C. Kojima (Graduate School of Biological Science, Nara Institute of Science and Technology) and Dr. T. Fujita (The Tokyo Metropolitan Institute of Medical Science) for helpful discussions and comments on our manuscript.

REFERENCES

1. Sen, G. C., and Lengyel, P. (1992) *J. Biol. Chem.* **267,** 5017–5020
2. Samuel, C. (2001) *Clin. Microbiol. Rev.* **14,** 778–809
3. Sato, M., Suemori, H., Hata, N., Asagiri, M., Ogasawara, K., Nakao, K., Nakaya, T., Katsuki, M., Noguchi, S., Tanaka, N., and Taniguchi, T. (2000) *Immunity* **13,** 539–548
4. Nakaya, T., Sato, M., Hata, N., Asagiri, M., Suemori, H., Noguchi, S., Tanaka, N., and Taniguchi, T. (2001) *Biochem. Biophys. Res. Commun.* **283,** 1150–1156
5. Liu, R., Genin, P., Mamane, Y., and Hiscott, J. (2000) *Mol. Cell. Biol.* **20,** 6342–6353
6. Lin, R., Mamane, Y., and Hiscott, J. (1999) *Mol. Cell. Biol.* **19,** 2465–2474
7. Suhara, W., Yoneyama, M., Iwamura, T., Yoshimura, S., Tamura, K., Namiki, H., Aimoto, S., and Fujita, T. (2000) *J. Biochem. (Tokyo)* **128,** 301–307
8. Suhara, W., Yoneyama, M., Kitabayashi, I., and Fujita, T. (2002) *J. Biol. Chem.* **277,** 22304–22313
9. Yoneyama, M., Suhara, W., Fukuhara, Y., Fukuda, M., Nishida, E., and Fujita, T. (1998) *EMBO J.* **17,** 1087–1095
10. Fitzgerald, K. A., McWhirter, S. M., Faia, K. L., Rowe, D. C., Latz, E., Golenbock, D. T., Coyle, A. J., Liao, S. M., and Maniatis, T. (2003) *Nat. Immunol.* **4,** 491–496
11. Sharma, S., tenOever, B. R., Grandvaux, N., Zhou, G. P., Lin, R., and Hiscott, J. (2003) *Science* **300,** 1148–1151
12. Vilcek, J., and Sen., G. (1996) *Virology* 375–399
13. Takahasi, K., Suzuki, N. N., Horiuchi, M., Mori, M., Suhara, W., Okabe, Y., Fukuhara, Y., Terasawa, H., Akira, S., Fujita, T., and Inagaki, F. (2003) *Nat. Struct. Biol.* **10,** 922–927
14. Qin, B. Y., Liu, C., Lam, S. S., Srinath, H., Delston, R., Correia, J. J., Derynck, R., and Lin, K. (2003) *Nat. Struct. Biol.* **10,** 913–921
15. Price, E. R., Jin, M., Lim, D., Pati, S., Walsh, C. T., and McKeon, F. D. (1994) *Proc. Natl. Acad. Sci. U. S. A.* **91,** 3931–3935
16. Dove, S., Joung, J., and Hochschild, A. (1997) *Nature* **386,** 627–630
17. Hu, J. C., Kornacker, M. G., and Hochschild, A. (2000) *Methods* **20,** 80–94
18. Nagata, T., Kishi, H., Liu, Q. L., Yoshino, T., Matsuda, T., Jin, Z. X., Murayama, K., Tsukada, K., and Muraguchi, A. (2000) *J. Immunol.* **165,** 4281–4289
19. Montague, J. W., Hughes, F. M., Jr., and Cidlowski, J. A. (1997) *J. Biol. Chem.* **272,** 6677–6684
20. Lin, R., Heylbroeck, C., Pitha, P. M., and Hiscott, J. (1998) *Mol. Cell. Biol.* **18,** 2986–2996
21. Servant, M. J., Grandvaux, N., tenOever, B. R., Duguay, D., Lin, R., and Hiscott, J. (2003) *J. Biol. Chem.* **278,** 9441–9447
22. Iwamura, T., Yoneyama, M., Yamaguchi, K., Suhara, W., Mori, W., Shiota, K., Okabe, Y., Namiki, H., and Fujita, T. (2001) *Genes Cells* **6,** 375–388
23. Mori, M., Yoneyama, M., Ito, T., Takahashi, K., Inagaki, F., and Fujita, T. (2004) *J. Biol. Chem.* **279,** 9698–9702
24. Kay, J. E. (1996) *Biochem. J.* **314,** 361–385
25. Lopez-Ilasaca, M., Schiene, C., Kullertz, G., Tradler, T., Fischer, G., and Wetzker, R. (1998) *J. Biol. Chem.* **273,** 9430–9434
26. Leverson, J. D., and Ness, S. A. (1998) *Mol. Cell* **1,** 203–211
27. Rycyzyn, M. A., Reilly, S. C., O'Malley, K., and Clevenger, C. V. (2000) *Mol. Endocrinol.* **14,** 1175–1186
28. Rycyzyn, M. A., and Clevenger, C. V. (2002) *Proc. Natl. Acad. Sci. U. S. A.* **99,** 6790–6795
29. Mamane, Y., Sharma, S., Petropoulos, L., Lin, R., and Hiscott, J. (2000) *Immunity* **12,** 129–140

Journal of General Virology (2005), 86, 645–656 DOI 10.1099/vir.0.80479-0

Genetic variation and dynamics of hepatitis C virus replicons in long-term cell culture

Nobuyuki Kato,[1] Takashi Nakamura,[1] Hiromichi Dansako,[1] Katsuyuki Namba,[2] Ken-ichi Abe,[1] Akito Nozaki,[1] Kazuhito Naka,[1] Masanori Ikeda[1] and Kunitada Shimotohno[3]

Correspondence
Nobuyuki Kato
nkato@md.okayama-u.ac.jp

[1,2]Department of Molecular Biology[1] and First Department of Internal Medicine[2], Okayama University Graduate School of Medicine and Dentistry, 2-5-1 Shikata-cho, Okayama 700-8558, Japan

[3]Department of Viral Oncology, Institute for Virus Research, Kyoto University, 53 Kawara-cho Shogo-in, Sakyo-ku, Kyoto 606-8507, Japan

Hepatitis C virus (HCV) genomic sequences are known to vary widely among HCV strains, but to date there have been few reports on the genetic variations and dynamics of HCV in an experimental system of HCV replication. In this study, a genetic analysis of HCV replicons obtained in long-term culture of two HCV replicon cells (50-1 and 1B-2R1), which were established from two HCV strains, 1B-1 and 1B-2, respectively, was performed. One person cultured 50-1 cells for 18 months, and two people independently cultured 50-1 cells for 12 months. 1B-2R1 cells were also cultured for 12 months. The whole nucleotide sequences of the three independent replicon RNA clones obtained at several time points were determined. It was observed that genetic mutations in both replicons accumulated in a time-dependent manner, and that the mutation rates of both replicons were approximately $3{\cdot}0 \times 10^{-3}$ base substitutions/site/year. The genetic diversity of both replicons was also enlarged in a time-dependent manner. The colony formation assay by transfection of total RNAs isolated from both replicon cells at different time points into naïve HuH-7 cells revealed that the genetic mutations accumulating with time in both replicons apparently improved colony formation efficiency. Taken together, these results suggest that the HCV replicon system is useful for the analysis of evolutionary dynamics and variations of HCV. Using this replicon cell culture system, it was demonstrated further that neither ribavirin nor its derivative mizoribine accelerated the mutation rate or the increase in the genetic diversity of HCV replicon.

Received 29 July 2004
Accepted 30 November 2004

INTRODUCTION

Hepatitis C virus (HCV) infection frequently causes chronic hepatitis (Choo *et al.*, 1989; Kuo *et al.*, 1989), which progresses to liver cirrhosis and hepatocellular carcinoma (Ohkoshi *et al.*, 1990; Saito *et al.*, 1990). HCV belongs to the family *Flaviviridae*, whose genome consists of a positive-stranded RNA molecule of 9·6 kb and encodes a large polyprotein precursor of about 3000 aa residues (Kato *et al.*, 1990a; Tanaka *et al.*, 1995). This polyprotein is processed by a combination of the host and viral proteases into at least 10 proteins: the core, envelope 1 (E1), E2, p7, and non-structural protein 2 (NS2), NS3, NS4A, NS4B, NS5A and NS5B (Grakoui *et al.*, 1993; Hijikata *et al.*, 1991, 1993; Mizushima *et al.*, 1994). These HCV proteins not only function in virus replication but may also affect a variety of cellular functions, including gene expression, signal transduction and apoptosis (Bartenschlager & Lohmann, 2000; Kato, 2001).

The most characteristic feature of the HCV genome is its remarkable genetic diversity and variation. To date, more than 50 HCV genotypes have been identified worldwide (Bukh *et al.*, 1995; Simmonds, 1995; Tokita *et al.*, 1996). Each of these genotypes shows more than 20 % difference at the nucleotide level and more than 15 % difference at the amino acid level compared with any of the other genotypes, although the 5′ untranslated regions (5′ UTRs) and core protein-encoding regions are highly homologous among the 50 genotypes (homology of >90 %). Comparisons of HCV genomes that belong to a single genotype have revealed 5–8 % diversity in nucleotide sequences and 4–5 % diversity in amino acid sequences (Kato *et al.*, 1990b; Kato, 2001). An analysis of the genetic diversity among the HCV genomes in an individual revealed that the diversity in nucleotide sequences averaged 0·9 %, and distributed throughout

Supplementary material is available in JGV Online.

the genome except in the 5′ UTR (Tanaka *et al.*, 1992). This so-called 'quasispecies' nature of the HCV genome has generally been observed in a single patient with chronic hepatitis C (Kato *et al.*, 1992; Martell *et al.*, 1992). This remarkable genetic diversity of the HCV genome suggests that HCV frequently causes mutations of the viral genome.

To date, two groups have estimated the mutation rate of the HCV genome using specimens from a chimpanzee (interval of 8 years) and a patient (interval of 13 years) infected with HCV (Ogata *et al.*, 1991; Okamoto *et al.*, 1992). They estimated that the mutation rate of the HCV genome was $1{\cdot}4–1{\cdot}9 \times 10^{-3}$ base substitutions/site/year; however, it is not clear whether this value indicates the actual mutation rate of the HCV genome, because complicated quasispecies are generally observed in patients or chimpanzees infected with HCV *in vivo*. On the other hand, Major *et al.* (1999) used chimpanzees that received intrahepatic inoculation with a full-length HCV RNA, and they estimated that the mutation rate of the HCV genome was $1{\cdot}5 \times 10^{-3}$ base substitutions/site/year. However, such experiments on HCV replication in humans are ethically problematic. Thus, there have been few reports on the genetic variations of HCV in an experimental system of HCV replication because of the lack of reproducible and efficient HCV proliferation in cell culture (Kato & Shimotohno, 2000).

In 1999, an HCV replicon system carrying autonomously replicating HCV subgenomic RNA containing the NS3-NS5B regions derived from the strain Con-1 was first established by using a human hepatoma cell line, HuH-7 (Lohmann *et al.*, 1999). Since then, several additional replicon systems have been established (Ali *et al.*, 2004; Blight *et al.*, 2000, 2003; Ikeda *et al.*, 2002; Kato *et al.*, 2003a; Pietschmann *et al.*, 2002; Zhu *et al.*, 2003). In these systems, replicated HCV RNAs were detected by Northern blot analysis and the HCV proteins, which were produced, were detected by Western blot analysis. Therefore, HCV replicon systems are thought to be useful for the analysis of genetic variations and dynamics of HCV.

Recently, we also established two HCV replicons (50-1 and 1B-2R1) derived from two HCV strains, 1B-1 and 1B-2, respectively, using HuH-7 cells (Kato *et al.*, 2003b; Kishine *et al.*, 2002). The nucleotide sequences of the NS3-NS5B regions in the 50-1 replicon showed differences of 8·1 % from those in the 1B-2R1 replicon (Kato *et al.*, 2003b), although both HCV strains belonged to genotype 1b. In order to understand the genetic variations and dynamics of HCV, we performed genetic analysis of HCV replicons obtained in long-term culture of 50-1 and 1B-2R1 replicon cells (termed 50-1 and 1B-2R1 cells, respectively). Here, we show that the accumulation of genetic mutations and the acquisition of the genetic diversity among HCV replicons are time dependent. In addition, we evaluated the effect of ribavirin and mizoribine on the genetic variations and dynamics of HCV replicons.

METHODS

Cell cultures. 50-1 and 1B-2R1 cells were cultured in Dulbecco's modified Eagle's medium supplemented with 10 % fetal bovine serum and 300 μg G418 (Geneticine; Invitrogen) ml^{-1}. The HCV replicon cells were known to possess the G418-resistant phenotype, because neomycin phosphotransferase (Neo^R) was produced by the efficient replication of HCV replicon in the cells. Therefore, when an HCV replicon is excluded from the cells or its level is decreased, the cells are killed by the presence of G418. 50-1 cells were also cultured in the presence of 5 or 25 μM ribavirin (Sigma) or 25 μM mizoribine (Sigma). In general, these replicon cells were passaged every 4 days.

Northern blot analysis. Total RNA from the cultured cells were prepared using an RNeasy extraction kit (Qiagen). Total RNA (3 μg) was used to detect the HCV replicon RNA and β-actin mRNA. Northern blotting and hybridization were performed as described previously (Ikeda *et al.*, 2002; Kato *et al.*, 2003b). A digoxigenin-labelled, negative-sense RNA probe complementary to the NS5B region (positions 8935–9374 of the HCV genome) was used for the detection of the replicon RNA. A β-actin specific digoxigenin-labelled antisense RNA probe was used to check the amount of RNA. The synthetic RNA transcribed from pNSS1RZ2RU (Kato *et al.*, 2003b) (10^8 and 10^7 genome equivalents spiked into normal cellular RNA) was used to compare the level of replicon RNA. An RNA ladder (Invitrogen) was also used to mark the molecular length.

Western blot analysis. The preparation of cell lysates, SDS-PAGE and immunoblotting analysis with a PVDF membrane were performed as described previously (Hijikata *et al.*, 1993; Naganuma *et al.*, 2000). The antibodies used to examine the expression levels of HCV proteins were those against NS3 (Novocastra Laboratories) and NS5B (a generous gift from M. Kohara, Tokyo Metropolitan Institute of Medical Science, Japan). Anti-β-actin antibody (AC-15; Sigma) was also used to detect β-actin as an internal control. Immunocomplexes on the membranes were detected by enhanced chemiluminescence assay (Renaissance; Perkin-Elmer Life Sciences).

RT-PCR. To amplify HCV RNA RT-PCR was performed as described previously (Kato *et al.*, 2003b). Briefly, the total RNA (2 μg) obtained from the replicon cells was used as a template for reverse transcriptase using SuperScript II (Invitrogen). PCR using proofreading KOD-plus DNA polymerase (Toyobo) was performed separately in two parts; one part covered the 5′ UTR to the amino terminal of the NS3 region, and the other part covered the NS3 region to the NS5B region. The PCR yielded a 2033 bp fragment for the former part and a 6107 bp fragment for the latter part.

cDNA cloning and sequencing. The PCR products were subcloned into the *Xba*I site of pBR322MC (Kishine *et al.*, 2002), which was derived from pBR322 and contained the multiple cloning site of pUC19, as described previously (Kato *et al.*, 2003b). Plasmid inserts were sequenced in both the sense and antisense directions by using Big Dye terminator cycle sequencing on an ABI PRISM 310 genetic analyser (Applied Biosystems).

Molecular evolutionary analysis. Nucleotide sequences of the clones obtained by RT-PCRs from 50-1 and 1B-2R1 cells were analysed by the neighbour-joining analysis using the program GENETYX-MAC (Software Development).

RNA transfection and selection of G418-resistant cells. RNA transfection into Huh-7 cells was performed by electroporation as described previously (Lohmann *et al.*, 1999). Briefly, total RNA (80 μg) isolated from the replicon cells was electroporated into 5×10^6 HuH-7 cells, and then 1×10^5 or 3×10^5 cells were seeded into a 10 cm diameter dish. After 48 h, G418 was added to

0·3 mg ml^{-1}, and the medium was changed twice per week. After 3 weeks, the colonies obtained on the culture dish were stained with Coomassie brilliant blue as described previously (Naganuma *et al.*, 2004).

RESULTS

Efficient replication of HCV replicons is maintained in long-term cell culture

In order to prepare the specimens for the genetic analysis of 50-1 and 1B-2R1 replicons, three people independently cultured 50-1 cells; one person cultured for 18 months (M) (K cell culture line; MK) and the two people cultured for 12 months (D and N cell culture lines; MD and MN), and one person cultured 1B-2R1 cells for 12 months. Using the specimens obtained at several time points (after 0, 4, 6, 12 and 18 months in culture), the levels of replicon RNAs and HCV proteins were examined by Northern and Western blot analyses, respectively. As shown in Fig. 1(a), replicon RNAs approximately 8 kb long were detected in all specimens except those from the cured cells, from which the replicons had been eliminated from the replicon cells by treatment with interferon-α. The number of copies of replicon RNAs in total RNA (each 3 μg) extracted from the replicon cells was estimated to be in the range of 10^7 to 10^8 by comparing these replicon RNAs with replicon RNA synthesized *in vitro*. The NS3 and NS5B were also detected in all specimens except those from the cured cells (Fig. 1b). The expression levels of replicon RNAs and HCV proteins differed somewhat among these specimens, and no strong quantitative relationship between replicon RNA and HCV proteins was observed (Fig. 1). These results suggest that the stability of replicon RNA or HCV proteins produced from the replicon RNA, or the efficiency of translation, changes during the periods of cell culture. In summary, we demonstrated that the replication efficiencies of the 50-1 and 1B-2R1 replicons remained high under the G418 selection pressure.

Sequence analysis of the 50-1 and 1B-2R1 replicon RNAs

To clarify the genetic variations and diversities of the replicons during the period of cell culture, we carried out sequence analysis of 50-1 and 1B-2R1 replicon RNAs obtained at several time points in the cultures of both replicon cells. Two separate RNA fragments (one was 2·0 kb in length, containing the 5′ UTR to the amino-terminal of the NS3 region; the other was 6·1 kb in length, containing the NS3 to NS5B regions) were amplified by RT-PCR, and three independent clones of each were sequenced after subcloning into pBR322MC, as described previously (Kato *et al.*, 2003b).

Genetic variations of 50-1 and 1B-2R1 replicons during long-term cell culture

The determined nucleotide sequences of the 50-1 and 1B-2R1 replicon RNAs were compared with those of the

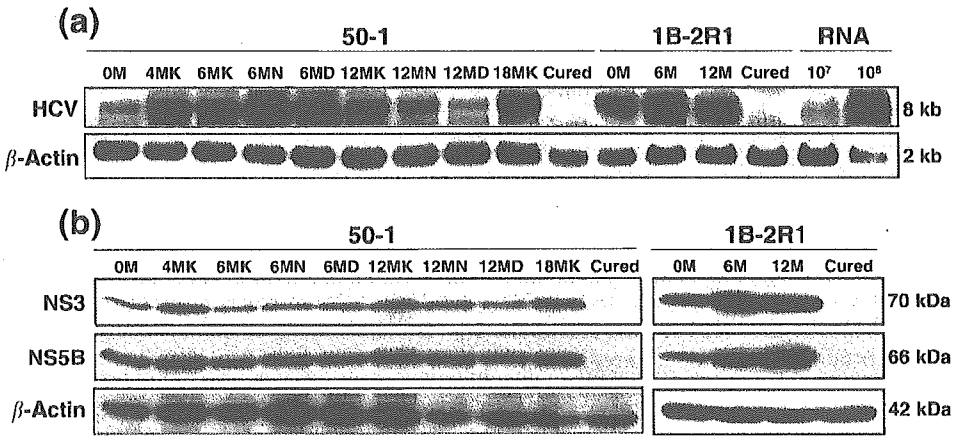

Fig. 1. Characterization of replicon cells in long-term cell culture. (a) Northern blot analysis. Total RNAs from 50-1 cells after 4 months (4MK), 6 months (6MK, 6MN and 6MD), 12 months (12MK, 12MN and 12MD) and 18 months (18MK) in culture, as well as total RNA from the parental 50-1 cells (0M) were used for the analysis. Total RNAs from 1B-2R1 cells after 6 months (6M) and 12 months (12M) in culture, as well as total RNA from the parental 1B-2R1 cells (0M) were used for the analysis. Total RNAs from each cured cells obtained from 50-1 and 1B-2R1 cells by interferon treatment were also used as a negative control. Northern blot analysis was performed using a positive-stranded HCV genome-specific RNA probe (upper panel) and a β-actin-specific probe (lower panel). Synthetic RNA transcribed from pNSS1RZ2RU (10^8 and 10^7 genome equivalents spiked into normal cellular RNA) was used for the comparison of the expression level. (b) Western blot analysis. The orders of specimens were the same as in (a). Productions of NS3 and NS5B in 50-1 and 1B-2R1 cells were analysed by immunoblotting using anti-NS3 and anti-NS5B antibodies, respectively. β-Actin was used as a control for the amount of protein loaded per lane.

original 50-1 (Kishine *et al.*, 2002; GenBank accession no. AB041927) and 1B-2R1 replicons (Kato *et al.*, 2003b; AB109543), respectively. The results revealed that the numbers of base substitutions in the first 2·0 kb region and in the NS region (6·1 kb) of both replicon RNAs were time-dependently increased with linearity (Fig. 2). These substitutions were considered to be mutations that occurred during the intracellular replication of replicon RNA. Based on the results after 12 months in culture, the apparent mutation rates in 50-1 replicon RNA were calculated to be $3{\cdot}1 \times 10^{-3}$ and $3{\cdot}0 \times 10^{-3}$ base substitutions/site/year in the first 2 kb region and NS region, respectively, indicating that there was no difference in mutation rate between the two regions of 50-1 replicon RNA. Interestingly, almost the same mutation rates ($3{\cdot}0 \times 10^{-3}$ base substitutions/site/year in the first 2 kb region; $3{\cdot}1 \times 10^{-3}$ base substitutions/site/year in NS region) were obtained for the 1B-2R1 replicon RNA, suggesting that the replication efficiency of the 1B-2R1 replicon was almost equal to that of the 50-1 replicon.

Fig. 3(a) shows the schematic presentation of mutations detected in the first 2 kb region by comparison with the original sequences (NNRZ2RU) of 50-1 and 1B-2R1 replicon RNAs (Kato *et al.*, 2003b; Kishine *et al.*, 2002). The results revealed that there were no common mutations among the four cell culture lines (three for 50-1 and one for 1B-2R1) over at least 12 months of cell culture. However, genetic mutations in both replicons were time-dependently increased and accumulated, and several mutations became abundant during the subsequent cell culture (Fig. 3a).

The NS regions (6·1 kb) of the 50-1 and 1B-2R1 replicon RNAs were also analysed in addition to the first 2 kb region. The mutation sites that showed amino acid substitutions are schematically presented in Fig. 3(b). Regarding the 50-1 replicon, 2 aa substitutions (P1115L and E1966A) were newly detected after 6 months in culture in all three cell culture lines, in addition to 2 aa substitutions (K1609E and V1896F) already observed when the replicon was first established. These four substituted amino acids were stably maintained over at least 12 months of cell culture. However, such amino acid substitutions were not observed in the 1B-2R1 replicon even after 12 months of culture. After more than 12 months in culture, several culture line-specific amino acid substitutions (*1–5 for the K culture line; *6–8 for the D culture line; and *9–12 for the N culture line in Fig. 3b) were observed in the 50-1 replicon. Also in the 1B-2R1 replicon, 1 aa substitution (*13 in Fig. 3b) was detected after 12 months in culture; however, no common amino acid substitutions were observed between the 50-1 and 1B-2R1 replicons. The mean numbers of amino acid substitutions occurring after 6 and 12 months in culture were 4·2 and 8·9, respectively, for the 50-1 replicon, and 4·7 and 10·0, respectively, for the 1B-2R1 replicon. These values indicate a steady genetic evolution of 50-1 and 1B-2R1 replicons during the cell culture.

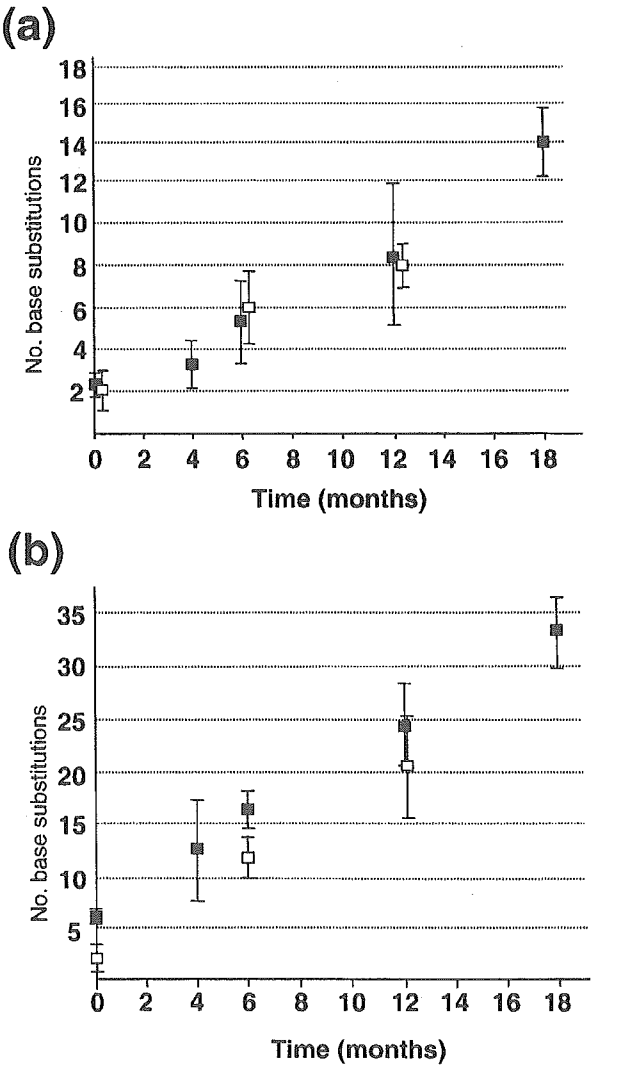

Fig. 2. Genetic variations of 50-1 and 1B-2R1 replicon RNAs. (a) First 2·0 kb region of replicon RNA. Filled squares indicate the mean numbers of base substitutions detected in nine (after 0, 6 and 12 months in culture) or three (after 4 and 18 months in culture) clones containing the first 2·0 kb region of 50-1 replicon RNA, by comparison with its original sequences (NNRZ2RU) (Kishine *et al.*, 2002). Open squares indicate the mean numbers of base substitutions detected in three clones containing the first 2·0 kb region of 1B-2R1 replicon RNA, by comparison with its original sequences (NNRZ2RU) (Kishine *et al.*, 2002). (b) NS region (6·1 kb) of replicon RNA. Filled squares indicate the mean numbers of base substitutions detected in nine (after 0, 6 and 12 months in culture) or three (after 4 and 18 months in culture) clones containing the NS region of 50-1 replicon RNA, by comparison with its original sequences (Kishine *et al.*, 2002). Open squares indicate the mean numbers of base substitutions detected in three clones containing the NS region of 1B-2R1 replicon RNA, by comparison with its original sequences (Kato *et al.*, 2003b).

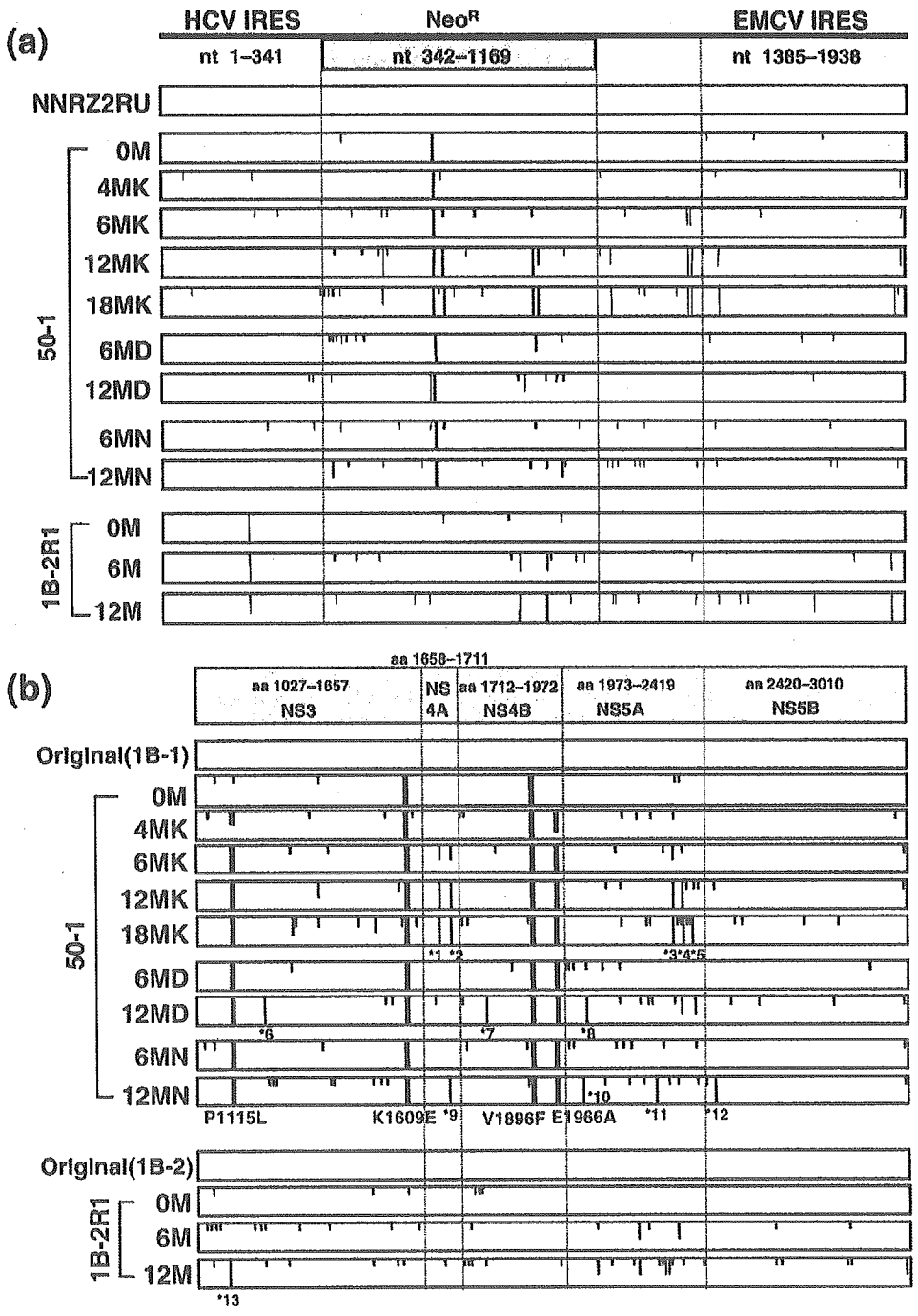

Fig. 3. Genetic variations of 50-1 and 1B-2R1 replicons in long-term cell culture. (a) Schematic presentation of mutations detected in first 2·0 kb regions of the replicon RNAs. Compared with the nucleotide sequences of the first 2·0 kb region of the original replicon RNA (NNRZ2RU), nucleotide positions mutated in all three clones, in two of three clones and in one of three clones are indicated by full-length, two-thirds and one-third vertical lines, respectively. Non-synonymous substitutions in the Neo^R region are indicated by heavy vertical lines. (b) Schematic presentation of amino acid substitutions detected in the NS regions of the replicons. Compared with the amino acid sequences of NS region of the original 50-1 (Kishine *et al.*, 2002) and 1B-2R1 replicons (Kato *et al.*, 2003b), amino acid positions substituted in all three clones, in two of three clones and in one of three clones are indicated by full-length, two-thirds and one-third vertical lines, respectively. Four amino acid substitutions (P1115L, K1609E, V1896F and E1966A) are indicated by heavy vertical lines. Culture line-specific amino acid substitutions (indicated by the numbers with asterisks) are as follows: *1, I1686V; *2, L1701R; *3, T2332A; *4, G2336E; *5, A2372T; *6, A1243G; *7, I1797V; *8, S2053G; *9, L1701R; *10, T2051N; *11, R2279G; *12, L2476M; *13, I1097V.

Classification of mutations occurring in 50-1 and 1B-2R1 replicon RNAs during the long-term cell culture

To understand the mutation mode of the replicons in long-term cell culture, we examined the numbers of synonymous and non-synonymous mutations with transition or transversion. The results are summarized in Table 1. The ratio of synonymous to non-synonymous mutations in 50-1 replicon RNA was 0·81 to 1·50 (1·38 ± 0·14 after 6 months in culture and 1·03 ± 0·20 after 12 months in culture), and the ratio in 1B-2R1 replicon RNA was 0·63 after 6 months in culture and 0·59 after 12 months in culture. These values indicate that amino acid substitutions in the replicons occur frequently during the cell culture. The rate of mutations with transition in the 50-1 replicon was 1·82–4·06-fold (2·00 ± 0·18 after 6 months in culture and 2·85 ± 1·07 after 12 months in culture) greater than the rate of mutations with transversion. Similarly, the 1B-2R1 replicon showed a transition-to-transversion ratio of 2·69 (after 6 months in culture) or 2·86 (after 12 months in culture).

Regarding the mutation patterns over more than 12 months of culture, we observed that A→G and U→C mutations were the most and second-most common mutations, and these mutations were approximately two to three times more common than G→A and C→U mutations (Supplementary Table A, which is available as Supplementary material in JGV Online). The rarest mutation was G→U (Supplementary Table A).

Genetic diversity of the 50-1 and 1B-2R1 replicons arising during long-term cell culture

To clarify whether or not the replicons acquire a quasispecies nature during long-term cell culture, we estimated the genetic diversities of the 50-1 and 1B-2R1 replicon populations. First, based on the sequence data of all clones obtained in this study, we constructed phylogenetic trees for the first 2 kb region and the NS region. The results revealed that the genetic diversity of 50-1 replicon populations was expanded in a time-dependent manner (Fig. 4). Similar phylogenetic trees were obtained for the 1B-2R1 replicon populations as well (data not shown). Next, as another index of genetic diversity, we calculated the mean number of nucleotide differences among three independent clones at each time point. The schematic presentation of such analysis on the NS regions of 50-1 and 1B-2R1 replicon RNAs was shown in Supplementary Fig. A, which is available as Supplementary material in JGV Online. The results also showed a time-dependent expansion of genetic diversity. After 12 months in culture, 0·32 % (mean of three cell culture lines) and 0·55 % diversities in nucleotide sequences were observed in the NS region of 50-1 and 1B-2R1 replicon RNAs. A similar time-dependent expansion of genetic diversity was also observed in the first 2 kb regions of both replicon RNAs (data not shown). These results indicate that the quasispecies nature of replicon RNA was easily acquired during the replication of the replicons.

Table 1. Base substitutions occurring in 50-1 and 1B-2R1 replicon RNAs during long-term cell culture

The counting of base substitutions was performed by comparison with the consensus sequence obtained from the 0M series of 50-1 or 1B-2R1 replicon.

Replicon	series	No. base substitutions										Synonymous/ non-synonymous	Transition/ transversion
		Transition					Transversion						
		Synonymous		Non-synonymous		Non-coding region	Synonymous		Non-synonymous		Non-coding region		
		Neo^R	NS	Neo^R	NS		Neo^R	NS	Neo^R	NS			
50-1	4MK	1	13	0	8	4	0	5	0	6	2	1·36	2·00
	6MK	0	20	2	10	8	3	8	1	9	1	1·41	1·82
	12MK	3	29	6	19	13	4	9	4	9	2	1·18	2·50
	18MK	5	43	8	26	16	3	10	4	14	5	1·17	2·72
	6MD	3	20	3	9	2	0	5	4	7	1	1·22	2·18
	12MD	5	29	2	26	3	2	5	1	8	0	1·11	4·06
	6MN	2	19	2	8	3	2	4	0	8	3	1·50	2·00
	12MN	3	25	2	21	9	1	6	5	15	3	0·81	2·00
1B-2R1	6M	1	14	5	14	1	1	1	3	5	3	0·63	2·69
	12M	2	22	4	29	6	1	2	3	10	6	0·59	2·86

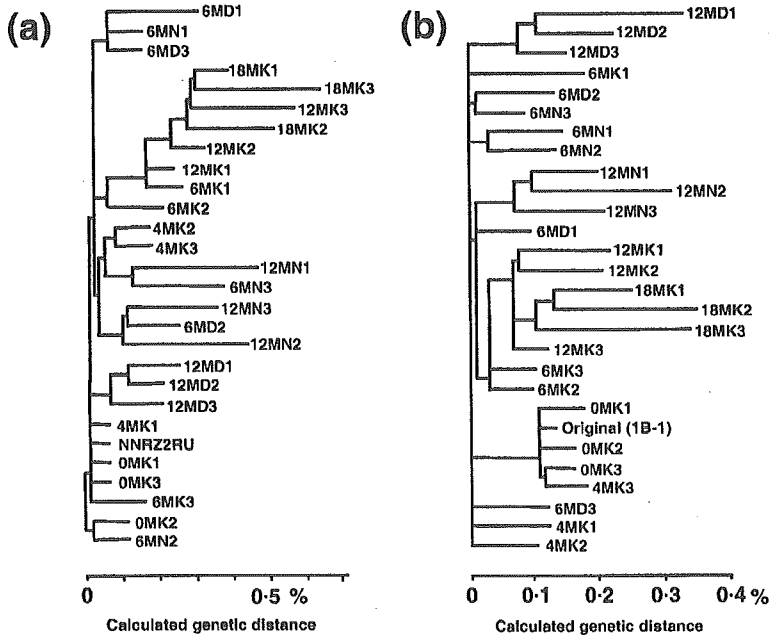

Fig. 4. Phylogenetic trees of 50-1 replicon populations obtained in long-term cell culture. The phylogenetic tree is depicted on the basis of nucleotide sequences of all replicon clones obtained by long-term culture of 50-1 cells. (a) The first 2·0 kb region of replicon RNA. NNRZ2RU indicates the original sequences of 50-1 replicon RNA, and the others indicate the names of clones. (b) The NS region of replicon RNA. Original (1B-1) indicates the original sequences of 50-1 replicon RNA, and the others indicate the names of clones.

Enhancement of HCV replication is associated with the expansion of the replicons' genetic diversity

To assess whether or not the mutations accumulating in the replicons increase the replication efficiencies of the replicons, the efficiency of colony formation (ECF) of the replicon was examined at each time point of the culture. An ECF assay was performed by transfection of total RNAs isolated from 50-1 and 1B-2R1 replicon cells at different time points into naïve HuH-7 cells. After 3 weeks of G418 selection, only a few colonies were obtained when RNAs from 50-1 replicon cells cultured less than 4 month were used (Fig. 5). However, ECF was apparently increased when RNAs from cells cultured 6 months, in particular the D and N cell culture lines, were used, and much higher numbers of colonies were obtained when RNAs from cells cultured 12 months were used (Fig. 5). Interestingly, ECFs of RNAs from D and N cell lines cultured more than 6 months were higher than those in the K cell culture line. These results indicated that ECF of the replicon was increased with the cultured periods of the replicon cells and suggested that ECF enhancement is associated with the expansion of the 50-1 replicon's genetic diversity.

In contrast to the case with 50-1 replicon cells, a number of colonies were obtained even when RNA from the initial culture of 1B-2R1 replicon cells was used (Fig. 5). In this replicon also, the ECF of RNA from cells cultured 12 months was apparently higher than those of RNA from the initial culture or 6 months of culture (Fig. 5). These results suggest that S2200R substitution, which was detected when the 1B-2R1 replicon was established (Kato *et al.*, 2003b), function as an adaptive mutation, and that the expansion of genetic diversity in the 1B-2R1 replicon also contributes to the enhancement of ECF, as was the case with the 50-1 replicon.

Effect of ribavirin and mizoribine on the genetic evolution and dynamics of the 50-1 replicon

Combined treatment of interferon plus ribavirin for patients with chronic hepatitis C has been shown to be more effective than treatment with interferon alone (McHutchison *et al.*, 1998), although it has been shown that ribavirin alone does not cause a decrease of HCV level in patients with chronic hepatitis C. Recently, several groups have reported that ribavirin might cause 'error catastrophe' of HCV genome (Contreras *et al.*, 2002; Tanabe *et al.*, 2004; Zhou *et al.*, 2003), however, controversial results have also been reported (Schinkel *et al.*, 2003). Therefore, to clarify whether or not ribavirin affects the genetic alterations of HCV, we cultured parent 50-1 cells (corresponding to 0M in Fig. 1) for 6 months in the presence of ribavirin (5 or 25 μM) or its derivative molecule, mizoribine (25 μM). As a control, the parent 50-1 cells were also cultured for 6 months in the absence of ribavirin or mizoribine. After 6 months in culture, the levels of replicon RNAs and HCV proteins were examined by Northern and Western blot analyses, respectively. As shown in Fig. 6(a), the level of replicon RNA in the cells treated with ribavirin or mizoribine was almost the same as that in the cells without ribavirin or mizoribine treatment. The NS3 and NS5B were also expressed at similar levels in the cells irrespective of ribavirin or mizoribine treatment (Fig. 6b). These results indicate that even 6 months of treatment with ribavirin or mizoribine did not prevent the replication of replicon RNA under the G418 selection pressure. Using the 50-1 cells cultured for 6 months with or without ribavirin or mizoribine, we performed sequence analysis of replicon

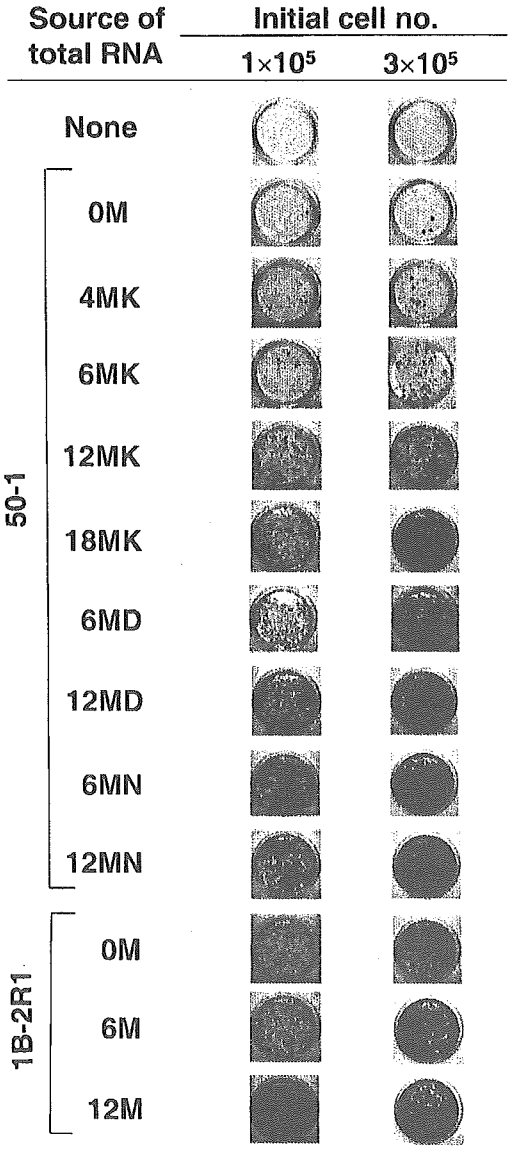

Fig. 5. ECF of the RNAs isolated from 50-1 and 1B-2R1 replicon cells at different time points in the culture. Total RNAs obtained from the replicon cells were transfected into HuH-7 cells as described in Methods. The panels show the cell colonies that were recovered after 3 weeks of G418 selection.

RNAs as described above. As shown in Table 2, the results revealed that the numbers of mutations in the first 2·0 kb and NS regions of the replicon RNAs sequenced were not significantly different among the specimens, although the number in the NS region derived from the cells treated with 25 μM of ribavirin was a little lower than those of the other specimens. These results suggest that the treatment of replicon cells with either ribavirin or mizoribine does not increase the mutation rate of replicon RNA. The ratio of synonymous and non-synonymous mutations, and the ratio

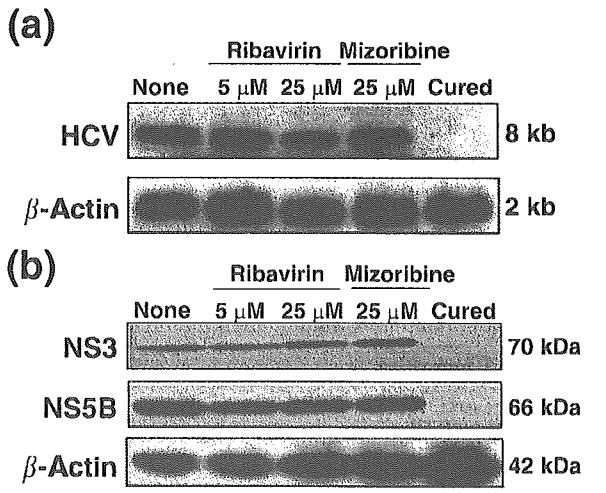

Fig. 6. Characterization of 50-1 cells cultured for 6 months in the presence of ribavirin or mizoribine. (a) Northern blot analysis. Total RNAs from 50-1 cells cultured for 6 months in the presence of ribavirin (5 and 25 μM) or mizoribine (25 μM), as well as total RNA from 50-1 cells cultured for 6 months in the absence of ribavirin and mizoribine were used for the analysis. Northern blot analysis was performed as indicated in Fig. 1(a). (b) Western blot analysis. The orders of specimens were the same as in (a). Western blot analysis was performed as indicated in Fig. 1(b).

of transition and transversion mutations were also not altered by ribavirin or mizoribine treatment (data not shown). In addition, we did not observe any ribavirin- or mizoribine-specific common amino acid substitutions in either the first 2 kb or NS regions of the replicon RNA, although P1115L and E1966A were detected after 6 months in culture in all cell culture lines. The above-described analysis of genetic diversity among the replicon RNAs did

Table 2. Base substitutions occurred in 50-1 replicon RNA during 6 months culture in the presence of ribavirin or mizoribine

6MR5 and 6MR25 indicate the series treated with 5 and 25 μM of ribavirin, respectively. 6MM25 indicates the series treated with 25 μM of mizoribine. The counting of base substitutions was performed by the comparison with the original sequence of 50-1 replicon (Kishine *et al.*, 2002).

Series	First 2-kb region	NS region
6M (Fig. 2)	5·4±1·9*	16·4±1·8
6M	5·7±2·5	16·0±0·0
6MR5	5·7±1·5	16·3±1·5
6MR25	5·7±1·5	10·7±1·2
6MM25	3·7±0·6	18·7±4·0

*Numbers of base substitutions±SD.

not reveal any significant differences between the specimens derived from the replicon cells with and those without ribavirin or mizoribine treatment (data not shown). Taken together, these results suggest that neither ribavirin nor mizoribine accelerated the mutation rate of HCV replicons or the development of their quasispecies nature.

DISCUSSION

In this study, we analysed the genetic evolution and dynamics of HCV replicons, and time-dependent genetic mutations of HCV replicons were observed. Time-dependent expansions of their genetic diversities were also revealed. Our results should provide useful fundamental information for understanding the remarkable genetic diversity and variation among the HCV genomes observed in patients with chronic hepatitis C.

Although RT-PCR techniques were used to amplify the replicon RNAs in this study, it is unlikely that the detected mutations were due to errors related to the use of the KOD-plus DNA polymerase in the PCR reaction, because we previously showed that KOD-plus DNA polymerase possessed a high proofreading activity (Alam *et al.*, 2002; Naganuma *et al.*, 2004). Furthermore, in the present study, we sequenced several clones (containing a 2·0 or 6·1 kb fragment) obtained by PCR using KOD-plus DNA polymerase and a single sequenced clone as a template, but no mutations were detected in these sequenced clones, indicating that KOD-plus DNA polymerase possesses extremely high fidelity. However, we are not able to completely exclude the possibility that some substitutions resulted from the erroneous use of KOD-plus DNA polymerase during the PCR. Even if such errors occurred, the error frequency is estimated to be less than one nucleotide per sequenced clone. This is explained as follows. Fig. 2 shows that the numbers of substitutions time-dependently increased with linearity in both HCV replicons. Interestingly, when these linear lines are extrapolated to zero base substitutions, the crossing points show approximately −2–−3 months in the time axis. These range of months is in accord with the time of initial electroporation of HCV replicon RNA to HuH-7 cells. Therefore, PCR-induced mutations are considered to be very rare and such mutations would have very little effect on the results shown in Fig. 2. In addition, to avoid a sampling effect, we sequenced three independent clones derived from each time point.

We showed that the mutation rates for the 50-1 and 1B-2R1 replicon RNAs were almost the same – about 3×10^{-3} base substitutions/site/year. However, the actual mutation frequency of the replicon RNAs would be higher than this value, because the mutations that occurred in positions that were critical for the replication of replicon RNA should not have been passed on to the progeny. Our observed mutation rates of the replicon RNAs were approximately two times higher than those previously obtained in chimpanzees and clinical patients with chronic hepatitis C (Major *et al.*, 1999; Ogata *et al.*, 1991; Okamoto *et al.*, 1992). Since the selective pressure of the immune system also functions *in vivo* (Kato *et al.*, 1993), the mutation rate in cell culture obtained in this study may be reasonable value as a potential mutation rate of HCV. However, direct comparison of these mutation rates would be difficult, because both the experimental model and analytical method were different in this study compared with the previous studies. It would be interesting to examine whether this mutation rate (3×10^{-3} base substitutions/site/year) would be maintained during longer-term culture of the replicon cells. If so, approximately 3 % of nucleotide sequences of the replicon RNAs might be mutated after 10 years in cell culture. Alternatively, the mutations might become saturated during further long-term culture of the replicon cells. To clarify this point, further long-term culture of replicon cells is in progress.

Although the mutations detected in this study were dispersed throughout the entire length of the replicon RNAs (Fig. 3), the mutation frequencies in the 5′ UTR and NS5B region were lower than those in other regions, and the NS5A region showed the highest mutation frequency. These observations are consistent with the genetic diversities of HCVs in patients with chronic hepatitis C reported to date (Kato, 2001). In addition, the positions in which amino acid substitutions were observed during the cell culture did not appear to be critical for replication of the HCV genome.

Time-dependent expansions of genetic diversities of HCV replicons were also found in this study. However, this finding seems to be different from the previous findings that HCV populations in the cells infected *in vitro* gradually altered with time and converged to the limited populations (Kato *et al.*, 1998; Kato, 2001). This gap may have been due to the differences in the HCV sources used: a patient's inoculum containing a quasispecies of HCV was used for the *in vitro* infection experiment, and a single HCV species was used for the replicon system. Alternatively, the gap may have been due to the overwhelming difference between the replication level of the HCV genome in the cells infected *in vitro* and that in the replicon cells.

To date, a number of amino acid substitutions belonging to adaptive mutations that enhance the frequency with which the replicon is established *in vitro* have been found in established HCV replicons (Bartenschlager, 2002; Blight *et al.*, 2000, 2003; Ikeda *et al.*, 2002; Krieger *et al.*, 2001; Lanford *et al.*, 2003; Lohmann *et al.*, 2001, 2003; Pflugheber *et al.*, 2002). Although none of the amino acid substitutions detected in the long-term cultures of the 50-1 and 1B-2R1 replicons were the same as those reported as adaptive mutations, ECF analysis of the replicons using naïve HuH-7 cells suggested that adaptive mutations accumulated in the replicon populations in a time-dependent manner. In particular, drastic enhancement of ECF was observed in the 50-1 replicon after 6 months of culture. However, this result suggests that the four common amino acid substitutions (P1115L, K1609E, V1896F and E1966A) do not contribute much to the drastic enhancement of ECF,

because the ECFs of 4MK and 6MK samples possessing these substitutions did not increase much. Therefore, we estimate that some uncommon amino acid substitutions accumulated as so-called adaptive mutations. The candidates for such adaptive mutations are culture-line-specific amino acid substitutions (Fig. 3b, *1–12), and many amino acid substitutions sporadically appeared in the replicons in the long-term cell cultures. To identify which amino acid substitution is the main contributor to the drastic enhancement of ECF, further transfection experiments using replicon RNAs possessing mutations will be needed. Based on the results of this study, S2200R substitution in the 1B-2R1 replicon is considered an adaptive mutation. This description is supported by the previous result that we were unable to obtain any G418-resistant colonies when the original 1B-2 replicon RNA library, used in the isolation of the 1B-2R1 replicon, was transfected into naïve HuH-7 cells (Kato *et al.*, 2003b). Since the ECF of 1B-2R1 replicon RNA from 12 months of culture was further enhanced, it may be that the I1097V substitution, detected commonly at 12 months of culture, functions as an additional adaptive mutation.

Interestingly, once a new mutation was observed in all three clones at a particular time point, the clones which went back to the original sequences were never obtained in the subsequent cell culture, except for one clone (a mutation in the HCV IRES region) derived from 1B-2R1 replicon cells after 12 months in culture (Fig. 3a). This finding suggests that the genetic evolution of HCV replicons is irreversibly progressing.

Although the mechanism of action of ribavirin for patients with chronic hepatitis C is ambiguous, an 'error catastrophe' theory of ribavirin has been proposed by several groups (Contreras *et al.*, 2002; Tanabe *et al.*, 2004; Zhou *et al.*, 2003). However, our results obtained in this study were not able to support this 'error catastrophe' theory, because ribavirin had no effect on the genetic variation and diversity of the 50-1 replicon. The concentration (5 and 25 μM) of ribavirin used in this study was considered to be reasonable, because the growth rate of 50-1 cells decreased at a ribavirin concentration of more than 50 μM, and approximately 10 μM of ribavirin is the maximum plasma concentration in current clinical usage (Tanabe *et al.*, 2004). Higher concentration (more than 50 μM) of ribavirin used in previous studies may be required for causation of the error catastrophe. Recently, a single amino acid substitution (F2834Y) was identified as a ribavirin-resistant NS5B mutation in genotype 1a (Young *et al.*, 2003); however, it is difficult to evaluate that finding in this study, because most of the HCV strains belonging to genotype 1b, including 1B-1 (50-1) and 1B-2 (1B-2R1), already possess a Tyr residue at position 2834. No amino acid substitution at position 2834 in NS5B was observed in the replicon cells treated with ribavirin.

This study provided the fact that the genetic diversity of HCV replicons was enlarged in a time-dependent manner during long-term cell culture. Since all the HCV replicons established to date have been shown to be highly sensitive to interferon-α, -β and -γ (Kato *et al.*, 2003b), and most of the HCV replicons established to date are able to replicate in only HuH-7 cells, the extensive genetic polymorphism of HCV replicon populations obtained by long-term cell culture may change the sensitivity against interferon or the ability of replication in the cells except for HuH-7. In the future, it will be necessary to clarify these points. Thus, HCV replicon populations obtained by long-term cell culture may be useful not only for analysis of the genetic variations and dynamics of HCV but also for analysis of the variable properties of HCV.

ACKNOWLEDGEMENTS

This work was supported by grants-in-aid for research on hepatitis from the Ministry of Health, Labour and Welfare of Japan and by grants-in-aid for scientific research from the Organization for Pharmaceutical Safety and Research (OPSR).

REFERENCES

Alam, S. S., Nakamura, T., Naganuma, A., Nozaki, A., Nouso, K., Shimomura, H. & Kato, N. (2002). Hepatitis C virus quasispecies in cancerous and noncancerous hepatic lesions: the core protein-encoding region. *Acta Med Okayama* **56**, 141–147.

Ali, S., Pellerin, C., Lamarre, D. & Kukolj, G. (2004). Hepatitis C virus subgenomic replicons in the human embryonic kidney 293 cell line. *J Virol* **78**, 491–501.

Bartenschlager, R. (2002). Hepatitis C virus replicons: potential role for drug development. *Nat Rev Drug Discov* **1**, 911–916.

Bartenschlager, R. & Lohmann, V. (2000). Replication of hepatitis C virus. *J Gen Virol* **81**, 1631–1648.

Blight, K. J., Kolykhalov, A. A. & Rice, C. M. (2000). Efficient initiation of HCV RNA replication in cell culture. *Science* **290**, 1972–1974.

Blight, K. J., McKeating, J. A., Marcotrigiano, J. & Rice, C. M. (2003). Efficient replication of hepatitis C virus genotype 1a RNAs in cell culture. *J Virol* **77**, 3181–3190.

Bukh, J., Miller, R. H. & Purcell, R. H. (1995). Genetic heterogeneity of hepatitis C virus: quasispecies and genotypes. *Semin Liver Dis* **15**, 41–63.

Choo, Q. L., Kuo, G., Weiner, A. J., Overby, L. R., Bradley, D. W. & Houghton, M. (1989). Isolation of a cDNA clone derived from a blood-borne non-A, non-B viral hepatitis genome. *Science* **244**, 359–362.

Contreras, A. M., Hiasa, Y., He, W., Terella, A., Schmidt, E. V. & Chung, R. T. (2002). Viral RNA mutations are region specific and increased by ribavirin in a full-length hepatitis C virus replication system. *J Virol* **76**, 8505–8517.

Grakoui, A., Wychowski, C., Lin, C., Feinstone, S. M. & Rice, C. M. (1993). Expression and identification of hepatitis C virus polyprotein cleavage products. *J Virol* **67**, 1385–1395.

Hijikata, M., Kato, N., Ootsuyama, Y., Nakagawa, M. & Shimotohno, K. (1991). Gene mapping of the putative structural region of the hepatitis C virus genome by *in vitro* processing analysis. *Proc Natl Acad Sci U S A* **88**, 5547–5551.

Hijikata, M., Mizushima, H., Tanji, Y., Komoda, Y., Hirowatari, Y., Akagi, T., Kato, N., Kimura, K. & Shimotohno, K. (1993). Proteolytic processing and membrane association of putative nonstructural proteins of hepatitis C virus. *Proc Natl Acad Sci U S A* **90**, 10773–10777.

Ikeda, M., Yi, M., Li, K. & Lemon, S. M. (2002). Selectable subgenomic and genome-length dicistronic RNAs derived from an infectious molecular clone of the HCV-N strain of hepatitis C virus replicate efficiently in cultured Huh7 cells. *J Virol* **76**, 2997–3006.

Kato, N. (2001). Molecular virology of hepatitis C virus. *Acta Med Okayama* **55**, 133–159.

Kato, N. & Shimotohno, K. (2000). Systems to culture hepatitis C virus. *Curr Top Microbiol Immunol* **242**, 261–278.

Kato, N., Hijikata, M., Ootsuyama, Y., Nakagawa, M., Ohkoshi, S., Sugimura, T. & Shimotohno, K. (1990a). Molecular cloning of the human hepatitis C virus genome from Japanese patients with non-A, non-B hepatitis. *Proc Natl Acad Sci U S A* **87**, 9524–9528.

Kato, N., Hijikata, M., Ootsuyama, Y., Nakagawa, M., Ohkoshi, S. & Shimotohno, K. (1990b). Sequence diversity of hepatitis C viral genomes. *Mol Biol Med* **7**, 495–501.

Kato, N., Ootsuyama, Y., Tanaka, T., Nakagawa, M., Nakazawa, T., Muraiso, K., Ohkoshi, S., Hijikata, M. & Shimotohno, K. (1992). Marked sequence diversity in the putative envelope proteins of hepatitis C viruses. *Virus Res* **22**, 107–123.

Kato, N., Sekiya, H., Ootsuyama, Y., Nakazawa, T., Hijikata, M., Ohkoshi, S. & Shimotohno, K. (1993). Humoral immune response to hypervariable region 1 of the putative envelope glycoprotein (gp70) of hepatitis C virus. *J Virol* **67**, 3923–3930.

Kato, N., Ikeda, M., Sugiyama, K., Mizutani, T., Tanaka, T. & Shimotohno, K. (1998). Hepatitis C virus population dynamics in human lymphocytes and hepatocytes infected in vitro. *J Gen Virol* **79**, 1859–1869.

Kato, T., Date, T., Miyamoto, M., Furusaka, A., Tokushige, K., Mizokami, M. & Wakita, T. (2003a). Efficient replication of the genotype 2a hepatitis C virus subgenomic replicon. *Gastroenterology* **125**, 1808–1817.

Kato, N., Sugiyama, K., Namba, K., Dansako, H., Nakamura, T., Takami, M., Naka, K., Nozaki, A. & Shimotohno, K. (2003b). Establishment of a hepatitis C virus subgenomic replicon derived from human hepatocytes infected in vitro. *Biochem Biophys Res Commun* **306**, 756–766.

Kishine, H., Sugiyama, K., Hijikata, M. & 7 other authors (2002). Subgenomic replicon derived from a cell line infected with the hepatitis C virus. *Biochem Biophys Res Commun* **293**, 993–999.

Krieger, N., Lohmann, V. & Bartenschlager, R. (2001). Enhancement of hepatitis C virus RNA replication by cell culture-adaptive mutations. *J Virol* **75**, 4614–4624.

Kuo, G., Choo, Q. L., Alter, H. J. & 17 other authors (1989). An assay for circulating antibodies to a major etiologic virus of human non-A, non-B hepatitis. *Science* **244**, 362–364.

Lanford, R. E., Guerra, B., Lee, H., Averett, D. R., Pfeiffer, B., Chavez, D., Notvall, L. & Bigger, C. (2003). Antiviral effect and virus-host interactions in response to alpha interferon, gamma interferon, poly(i)-poly(c), tumor necrosis factor alpha, and ribavirin in hepatitis C virus subgenomic replicons. *J Virol* **77**, 1092–1104.

Lohmann, V., Korner, F., Koch, J., Herian, U., Theilmann, L. & Bartenschlager, R. (1999). Replication of subgenomic hepatitis C virus RNAs in a hepatoma cell line. *Science* **285**, 110–113.

Lohmann, V., Korner, F., Dobierzewska, A. & Bartenschlager, R. (2001). Mutations in hepatitis C virus RNAs conferring cell culture adaptation. *J Virol* **75**, 1437–1449.

Lohmann, V., Hoffmann, S., Herian, U., Penin, F. & Bartenschlager, R. (2003). Viral and cellular determinants of hepatitis C virus RNA replication in cell culture. *J Virol* **77**, 3007–3019.

Major, M. E., Mihalik, K., Fernandez, J., Seidman, J., Kleiner, D., Kolykhalov, A. A., Rice, C. M. & Feinstone, S. M. (1999). Long-term follow-up of chimpanzees inoculated with the first infectious clone for hepatitis C virus. *J Virol* **73**, 3317–3325.

Martell, M., Esteban, J. I., Quer, J., Genesca, J., Weiner, A., Esteban, R., Guardia, J. & Gomez, J. (1992). Hepatitis C virus (HCV) circulates as a population of different but closely related genomes: quasispecies nature of HCV genome distribution. *J Virol* **66**, 3225–3229.

McHutchison, J. G., Gordon, S. C., Schiff, E. R. & 7 other authors (1998). Interferon alfa-2b alone or in combination with ribavirin as initial treatment for chronic hepatitis C. Hepatitis Interventional Therapy Group. *N Engl J Med* **339**, 1485–1492.

Mizushima, H., Hijikata, M., Tanji, Y., Kimura, K. & Shimotohno, K. (1994). Analysis of N-terminal processing of hepatitis C virus nonstructural protein 2. *J Virol* **68**, 2731–2734.

Naganuma, A., Nozaki, A., Tanaka, T., Sugiyama, K., Takagi, H., Mori, M., Shimotohno, K. & Kato, N. (2000). Activation of the interferon-inducible 2′-5′-oligoadenylate synthetase gene by hepatitis C core protein. *J Virol* **74**, 8744–8750.

Naganuma, A., Dansako, H., Nakamura, T., Nozaki, A. & Kato, N. (2004). Promotion of microsatellite instability by hepatitis C virus core protein in human non-neoplastic hepatocyte cells. *Cancer Res* **64**, 1307–1314.

Ogata, N., Alter, H. J., Miller, R. H. & Purcell, R. H. (1991). Nucleotide sequence and mutation rate of the H strain of hepatitis C virus. *Proc Natl Acad Sci U S A* **88**, 3392–3396.

Ohkoshi, S., Kojima, H., Tawaraya, H. & 8 other authors (1990). Prevalence of antibody against non-A, non-B hepatitis virus in Japanese patients with hepatocellular carcinoma. *Jpn J Cancer Res* **81**, 550–553.

Okamoto, H., Kojima, M., Okada, S. & 7 other authors (1992). Genetic drift of hepatitis C virus during an 8·2-year infection in a chimpanzee: variability and stability. *Virology* **190**, 894–899.

Pflugheber, J., Fredericksen, B., Sumpter, R., Jr, Wang, C., Ware, F., Sodora, D. L. & Gale, M., Jr (2002). Regulation of PKR and IRF-1 during hepatitis C virus RNA replication. *Proc Natl Acad Sci U S A* **99**, 4650–4655.

Pietschmann, T., Lohmann, V., Kaul, A., Krieger, N., Rinck, G., Rutter, G., Strand, D. & Bartenschlager, R. (2002). Persistent and transient replication of full-length hepatitis C virus genomes in cell culture. *J Virol* **76**, 4008–4021.

Saito, I., Miyamura, T., Ohbayashi, A. & 10 other authors (1990). Hepatitis C virus infection is associated with the development of hepatocellular carcinoma. *Proc Natl Acad Sci U S A* **87**, 6547–6549.

Schinkel, J., de Jong, M. D., Bruning, B., van Hoek, B., Spaan, W. J. & Kroes, A. C. (2003). The potentiating effect of ribavirin on interferon in the treatment of hepatitis C: lack of evidence for ribavirin-induced viral mutagenesis. *Antivir Ther* **8**, 535–540.

Simmonds, P. (1995). Variability of hepatitis C virus. *Hepatology* **21**, 570–583.

Tanabe, Y., Sakamoto, N., Enomoto, N. & 9 other authors (2004). Synergistic inhibition of intracellular hepatitis C virus replication by combination of ribavirin and interferon-alpha. *J Infect Dis* **189**, 1129–1139.

Tanaka, T., Kato, N., Nakagawa, M., Ootsuyama, Y., Cho, M. J., Nakazawa, T., Hijikata, M., Ishimura, Y. & Shimotohno, K. (1992). Molecular cloning of hepatitis C virus genome from a single

Japanese carrier: sequence variation within the same individual and among infected individuals. *Virus Res* **23**, 39–53.

Tanaka, T., Kato, N., Cho, M. J. & Shimotohno, K. (1995). A novel sequence found that at the 3′ terminus of hepatitis C virus genome. *Biochem Biophys Res Commun* **215**, 744–749.

Tokita, H., Okamoto, H., Iizuka, H., Kishimoto, J., Tsuda, F., Lesmana, L. A., Miyakawa, Y. & Mayumi, M. (1996). Hepatitis C virus variants from Jakarta, Indonesia classifiable into novel genotypes in the second (2e and 2f), tenth (10a) and eleventh (11a) genetic groups. *J Gen Virol* **77**, 293–301.

Young, K. C., Lindsay, K. L., Lee, K. J., Liu, W. C., He, J. W., Milstein, S. L. & Lai, M. M. (2003). Identification of a ribavirin-resistant NS5B mutation of hepatitis C virus during ribavirin monotherapy. *Hepatology* **38**, 869–878.

Zhou, S., Liu, R., Baroudy, B. M., Malcolm, B. A. & Reyes, G. R. (2003). The effect of ribavirin and IMPDH inhibitors on hepatitis C virus subgenomic replicon RNA. *Virology* **310**, 333–342.

Zhu, Q., Guo, J. T. & Seeger, C. (2003). Replication of hepatitis C virus subgenomes in nonhepatic epithelial and mouse hepatoma cells. *J Virol* **77**, 9204–9210.

Available online at www.sciencedirect.com

SCIENCE DIRECT®

Virology 331 (2005) 407–417

VIROLOGY

www.elsevier.com/locate/yviro

Suppression of hepatitis C virus replicon by TGF-β

Takayuki Murata, Takayuki Ohshima, Masashi Yamaji, Masahiro Hosaka, Yusuke Miyanari, Makoto Hijikata, Kunitada Shimotohno*

Department of Viral Oncology, Institute for Virus Research, Kyoto University, Sakyo-ku, Kyoto 606-8507, Japan

Received 24 July 2004; returned to author for revision 25 August 2004; accepted 20 October 2004

Abstract

Hepatitis C virus (HCV) is one of the major causative agents of liver diseases, such as liver inflammation, fibrosis, cirrhosis, and hepatocellular carcinoma. Using an efficient HCV subgenomic replicon system, we demonstrate that transforming growth factor-beta (TGF-β) suppresses viral RNA replication and protein expression from the HCV replicon. We further show that the anti-viral effect of this cytokine is associated with cellular growth arrest in a manner dependent on Smad signaling, not mitogen-activated protein kinase (MAPK) signaling. These results suggest a novel insight into the mechanisms of liver diseases caused by HCV.

Keywords: TGF-β; Hepatitis C virus; Replicon; Smad; MAPK

Introduction

Hepatitis C virus (HCV), a member of the *Flaviviridae* family, is an enveloped virus with a positive single-stranded 9.6-kb RNA genome (Murphy et al., 1995). The virus has been identified as the major causative agent of non-A, non-B hepatitis (Choo et al., 1989) that persistently infects several millions of people throughout the world. Although acute phase HCV infection is asymptomatic in most cases, the virus frequently establishes a persistent infection. This condition is associated with serious clinical diseases, including chronic hepatitis and liver fibrosis, which can lead to liver cirrhosis and eventually hepatocellular carcinoma (Goodman and Ishak, 1995).

Despite the clinical significance, molecular investigation of the virus has been hampered due to the lack of cell culture systems that efficiently support HCV replication. In 1999, the establishment of an HCV subgenomic replicon cell culture system (Lohmann et al., 1999) improved the situation. The subgenomic replicon RNA is composed of the HCV 5′-untranslated region (UTR) containing an internal ribosomal entry site (IRES), a neomycin phosphotransferase (*neo*) gene, the HCV nonstructural (NS) proteins 3 through 5B under the control of an encephalomyocarditis virus (EMCV) IRES, followed by the HCV 3′-UTR. The *neo* gene is expressed under the control of the HCV IRES, and thereby, gives the resistance to the cells in which replicon RNA exists. Instead of the *neo* gene, the luciferase gene can be used as a marker. Using the luciferase gene is beneficial in that it offers easy, speedy, and reliable detection. As the RNA replicates autonomously in cultured cells, this replicon system provides a unique tool for the analysis of the molecular mechanisms of HCV replication and the screening of anti-HCV compounds.

Transforming growth factor-beta (TGF-β) promotes the development of liver fibrosis and cirrhosis (Gressner et al., 2002); serum cytokine levels are associated with the severity of liver fibrosis in patients with chronic HCV (Nelson et al., 1997; Neuman et al., 2001; Tsushima et al., 1999). As high levels of TGF-β expression correlate with chronic hepatitis and cirrhosis (Calabrese et al., 2003; Shirai et al., 1994), cytokine serum concentrations serve as useful serologic markers for hepatitis, cirrhosis, and carcinoma (Song et al., 2002). Despite accumulating clinical observations, the direct effect of TGF-β on HCV replication remains unknown.

* Corresponding author. Fax: +81 75 751 3998.
E-mail address: kshimoto@virus.kyoto-u.ac.jp (K. Shimotohno).

0042-6822/$ - see front matter © 2004 Elsevier Inc. All rights reserved.
doi:10.1016/j.virol.2004.10.036

Molecular biological analyses have revealed that the cytokine is a multifunctional cytokine that regulates multiple biological functions, including cellular growth inhibition, extracellular matrix (ECM) formation, apoptosis, and cell differentiation (reviewed in Derynck and Zhang, 2003; Miyazono et al., 2000). Following receptor ligation, the activation of receptor-regulated Smad (R-Smad, Smad2, and Smad3) enhances complex formation with the common-mediator Smad (Co-Smad, Smad4). These complexes translocate to the nucleus, where they directly regulate the transcription of various target genes. TGF-β receptor ligation also activates members of the mitogen-activated protein kinase (MAPK) family, including p38 MAPK, c-Jun N-terminal kinase (JNK), and extracellular signal-regulated kinase (ERK).

In this study, we demonstrate that TGF-β inhibits HCV RNA replication and viral protein expression using a HCV subgenomic replicon system. The anti-viral effect of TGF-β was associated with growth arrest of cells and the activation of Smad, not MAPK, signaling. Our results provide insight into the mechanisms of liver disease pathogenesis caused by HCV.

Results

Construction of a highly efficient and sensitive replicon system

Although we had previously developed subgenomic HCV replicon cell lines (Kishine et al., 2002), we desired a highly efficient replicon system to study the molecular mechanisms of HCV replication. Among the G418-resistant subgenomic replicon cell lines, we identified a replicon cell clone (MH14) in which the viral RNA levels were higher than those in other replicon cells (Miyanari et al., 2003). The amount of replicon RNA present in MH14 cells was approximately five times greater than that present in typical MH5 replicon cells (Fig. 1B). The production of NS5A protein in MH14 cells was also greater (Fig. 1C), suggesting efficient replication of the viral RNA. Sequence analysis of replicon RNA in the MH14 cells revealed two point mutations; S2204R, the replacement of the Ser residue at position 2204 with Arg, and a silent mutation L1882L in the NS4B coding region, which did not encode an amino acid substitution. The S2204R mutation corresponded to a previously reported adaptive mutation in NS5A (Lohmann et al., 2003). At least two forms of NS5A, p56 (basally phosphorylated form), and p58 (hyper-phosphorylated form), have been reported. Residue Ser-2204 is important for hyper-phosphorylation of the protein (Tanji et al., 1995). As expected, only the basally phosphorylated p56 form was detected and hyper-phosphorylated p58 was missing in the MH14 cells, while MH5 cells, which do not carry a mutation at the sequences liable for the hyper-phosphorylation, produce both the p56 and p58 forms of NS5A (Fig. 1C).

To test permissiveness of MH14 cells for HCV replication, cells were cured of the HCV replicon RNA by prolonged treatment with IFN-α,resulting in the curedMH14 line (Figs. 1B, C). MH5 replicon cells were treated with IFN-α in parallel, for use as controls. To examine permissiveness, cured cells were transfected with replicon RNAs in which the firefly luciferase gene was inserted (Fig. 1A). We, here, used luciferase gene as a marker since it is more convenient and has the sensitivity for better quantitation. Cells were harvested at various time points after transfection and cellular luciferase activities were measured subsequently (Figs. 1D–F). Luciferase activity in transfected cells reflects the replication of the replicon RNA. Polymerase-defective RNA replicon constructs, in which the catalytic GDD motif of the NS5B polymerase was substituted to the inactive GHD motif, were used as negative controls. When cells were transfected with the prototype NN replicon RNA, luciferase activity decreased rapidly 3 to 5 days after transfection (Figs. 1D–F, NN). Use of the MH14 RNA, which is identical to the prototype NN RNA with the exception of the L1882L and S2204R mutations, resulted in higher luciferase activities (Figs. 1D–F, MH14) than those observed in cells transfected with the NN RNA. For the curedMH14 cells, luciferase activity did not decrease (Fig. 1F, MH14), but increased, peaking 3 to 5 days after transfection, suggesting highly efficient replication.

We also tested the effect of the mutations and cured cell lines on G418-resistance transduction efficiencies (not shown) and confirmed that the numbers of G418-resistant colonies exhibited a similar trend as seen for the luciferase activities described above.

These results suggest that the curedMH14 cells were highly permissive for replication of RNA containing the adaptive mutations.

Furthermore, when curedMH14 cells were transfected with the highest efficiency replicon RNA, high luciferase activity persisted for greater than 1 month (data not shown) in the absence of selection.

Suppression of HCV replicon with luciferase by TGF-β

As we have constructed a highly efficient and sensitive replicon system using a luciferase reporter and curedMH14 cells, we used this system to screen anti-HCV compounds. Treatment for 3 days with IFN-α, IL-1β, or cyclosporin A reduced the observed luciferase activities to 3.8%, 9.5%, or 3.4% of control levels, respectively (Fig. 2A). As all three treatments have been reported to repress HCV replicon (Blight et al., 2000; Watashi et al., 2003; Zhu and Liu, 2003), the system is an effective method to screen for potential anti-HCV drugs. We also observed the suppressive effect of TGF-β on luciferase activity (Fig. 2A). While treatment with 2 ng/ml TGF-β (Fig. 2B, open circle) for 36 h had little effect on luciferase activity, enzymatic activity decreased to 11%, 12%, 10% that of the mock-treated cells (black circle) at 48, 60, and 72 h, respectively. To examine

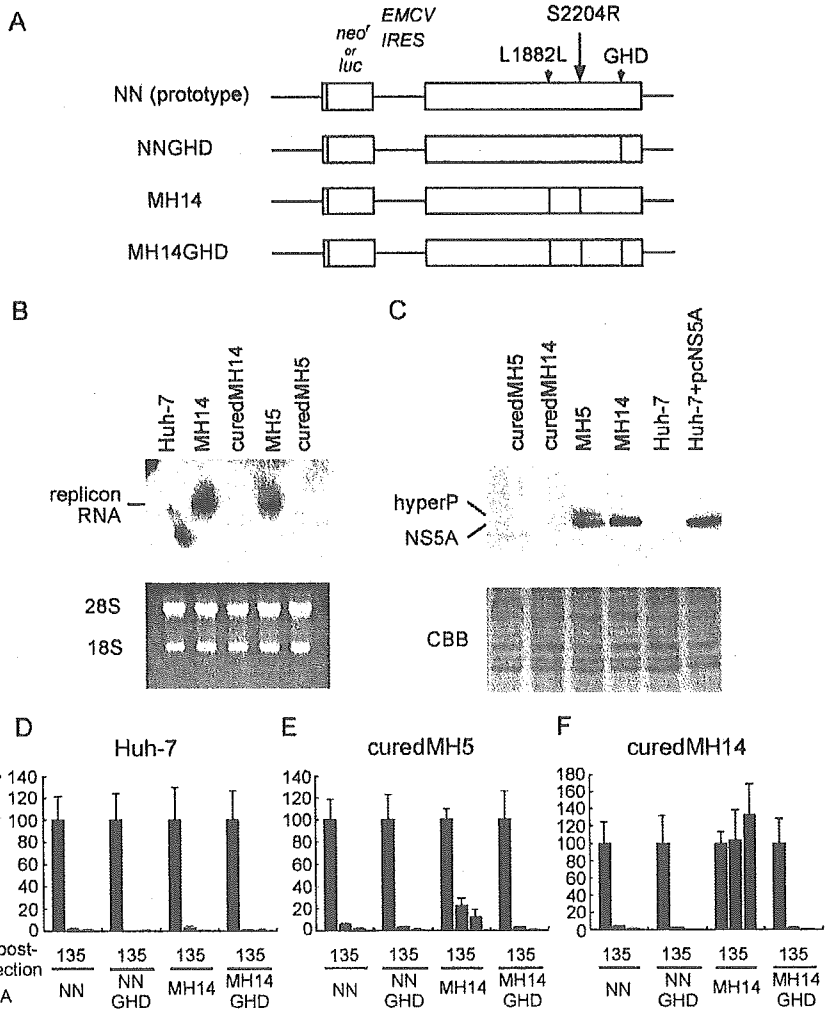

Fig. 1. Constructions and cells used in this study. (A) Schematic representation of the subgenomic replicon RNA constructs. The prototype NN RNA was used for transfection to obtain subgenomic replicon cell lines, including MH5 and MH14. NNGHD denotes polymerase-defective mutant, in which the catalytic GDD motif of the NS5B polymerase was substituted to the inactive GHD motif, and was used as a negative control. MH14 RNA carries two mutations, which were found in the replicon RNA in MH14 subgenomic replicon cells. MH14GHD is a negative control for the MH14 RNA. The ORFs are depicted as open boxes. The locations of the mutations introduced into the viral proteins are indicated by vertical lines. (B) Northern blot analysis of total RNA extracted from replicon cells. RNA from Huh-7, MH14, curedMH14, MH5, or curedMH5 cells was electrophoresed on denaturing agarose gels, blotted, and probed with an HCV RNA (upper panel). As an internal control, the ethidium bromide-staining pattern of 28S and 18S ribosomal RNA is shown (lower panel). (C) Western blot analysis of NS5A protein expressed in Huh-7, MH14, curedMH14, MH5, or curedMH5 cells (upper panel). As a control, wild-type NS5A protein was exogenously produced in Huh-7 cells from an expression plasmid (Huh-7 + pcNS5A). The position of the hyper-phosphorylated form of the protein is designated HyperP. As an internal control, the Coomassie brilliant blue (CBB) staining pattern of the same blot is shown (lower panel). (D–F) Replication of replicon RNAs with mutations in Huh-7 cells or its derivatives. Huh-7 (D), curedMH5 (E), or curedMH14 (F) cells were transfected with replicon RNA constructs containing the luciferase gene (depicted in A). Luciferase activity was measured at 1, 3, and 5 days after transfection. Each bar represents the mean and SD of three independent transfections.

the effect of TGF-β on luciferase expression and activity, the pCMV-Luc, in which the firefly luciferase gene is driven under the control of the CMV promoter, was used in Fig. 2C. While TGF-β treatment repressed the luciferase expression from replicon (Fig. 2B), we found that the cytokine enhanced the luciferase expression from the CMV promoter (Fig. 2C), provably because of the activation of transcriptional factors (Derynck and Zhang, 2003; Miyazono et al., 2000).

TGF-β is a multifunctional cytokine that exerts a range of biological activities, including cell growth inhibition (Derynck and Zhang, 2003; Miyazono et al., 2000). When exposed to TGF-β, cells generally arrest in the G(1)/S phase of the cell cycle. We, therefore, examined cell growth of curedMH14 cells (Fig. 2D). As expected, the growth of curedMH14 cells was partially inhibited by cytokine treatment (Fig. 2D, open circle). As assessed by FACS, administration of TGF-β for 2–3 days resulted in G(1)/S-arrest, while a 1-day treatment had no effect on cell cycle (Fig. 2E).

Fifty percent suppression of luciferase activity, after 3 days of treatment, was observed in the presence of